Development of Remote Sensing Techniques for the Implementation of Site-Specific Herbicide Management

Peter R. Eddy
B.Sc. University of Lethbridge, 2002

A Thesis

Submitted to the School of Graduate Studies

of the University of Lethbridge

in Partial Fulfillment of the

Requirements of the Degree

MASTER OF SCIENCE

Department of Geography
University of Lethbridge
LETHBRIDGE, ALBERTA CANADA

ABSTRACT

Selective application of herbicide in agricultural cropping systems provides both economic and environmental benefits. Implementation of this technology requires knowledge of the location and density of weed species within a crop. In this study, two image classification techniques (Artificial Neural Networks (ANNs) and Maximum Likelihood Classification (MLC)) are compared for accuracy in weed/crop species discrimination. In the summer of 2005, high spatial resolution (1.25mm) ground-based hyperspectral image data were acquired over field plots of three crop species seeded with two weed species. Image data were segmented using a threshold technique to identify vegetation for classification. The ANNs consistently outperformed MLC in single-date and multitemporal classification accuracy. With advancements in imaging technology and computer processing speed, these network models would constitute an option for real-time detection and mapping of weeds for the implementation of site-specific herbicide management.

ACKNOWLEDGEMENTS

I would like to acknowledge my graduate committee for making this research possible. Dr. Anne Smith (Research Scientist - Agriculture and Agri-Food Canada (AAFC) and Adjunct Professor - University of Lethbridge) is thanked for securing funding for this project and providing office/laboratory space and field equipment as well as countless hours of support and guidance throughout. I acknowledge Dr. Derek Peddle (Professor - University of Lethbridge) for his assistance, especially in the final preparation of this thesis and peer-review publications. Thanks to Dr. Craig Coburn (Assistant Professor - University of Lethbridge), for the many "blue skying" or should I say "*cyan* skying" sessions in his office and excellent comments and assistance in development of my scientific writing. Last but certainly not least, I would like to thank Dr. Robert Blackshaw (Research Scientist - AAFC and Adjunct Professor - University of Lethbridge) for sharing his expertise in weed science and lending his technical staff for field plot seeding and maintenance.

I would also like to acknowledge funding received through the graduate research affiliate program (AAFC) Improving Farming Systems and Practices program (AAFC) and the teaching assistantship program (University of Lethbridge). Neil James (Delta Tee Enterprises Ltd.) is thanked for development and troubleshooting of the sensor system and acquisition software. Special thanks to Dr. Bernie Hill (Research Scientist – AAFC) and his student April Banack for introducing me to the world of neural networks, model development and use of the Neuralware software package.

Finally I would like to extend my gratitude to my family; my love Sarah, mother Carol and sister Crystal for their unfailing support and talking me down off the ledge more than once. Thanks so much.

TABLE OF CONTENTS

LIST OF ACRONYMS

ANN – Artificial Neural Network

ANOVA – Analysis of Variance

CAN – Canola (*Brassica napus* L.)

CCD – Charge-Coupled Device

CCM – Colour Co-occurrence Method

DA – Discriminant Analysis

DN – Digital Number

EM – Electro-Magnetic

GIS – Geographic Information System

GPS – Global Positioning System

HSI – Hue, Saturation, Intensity

MCARI – Modified Chlorophyll Absorption Reflectance Index

MLC – Maximum-Likelihood Classification

MLP – Multi-Layer Perceptron

NDVI – Normalized Difference Vegetation Index

NIR – Near-Infrared

PCA – Principal Component Analysis

PEA – Field Pea (*Pisum sativum* L.)

RGB – Red, Green, Blue

ROI – Region of Interest

RS – Remote Sensing

RRP – Redroot Pigweed (*Amaranthus retroflexus* L.)

SDA – Stepwise Discriminant Analysis

SOM – Self-Organizing Map

SSHM – Site-Specific Herbicide Management

SZA – Solar Zenith Angle

VI – Vegetation Index

WHT – Spring Wheat (*Triticum aestivum* L.)

WO – Wild Oat (*Avena fatua* L.)

LIST OF FIGURES

LIST OF TABLES

CHAPTER 1 INTRODUCTION

Precision agricultural techniques aim to manage fields based on spatial variability rather than generalized surveyed boundaries. With the rapid development of spatial mapping technologies, these techniques have now become a reality. Agricultural fields are typically non-uniform as spatial variability in soil properties and topography exists within field boundaries. Through gathering and maintaining information about this spatial variability, management of agricultural inputs including fertilizer, irrigation and pesticides can be applied at varied rates to promote efficient use and optimize crop production (Mulla and Schepers, 1997).

Site-specific herbicide management (SSHM) is one facet of precision agriculture, where herbicide application is dependant upon zones of weed density within the field rather than full spatial coverage application (Thompson et al., 1991). For weed management, producers have three main options; mechanical control, chemical control or a combination of the two. Mechanical control involving tillage, with the exception of inter-row cultivation, is generally limited to pre-seeding or post-harvest situations in cropping operations. Research has linked tillage to soil erosion, the loss of soil moisture, and the spread of weed patches to other areas of the field (Brown and Steckler, 1995). With chemical management, a sprayer is typically used to apply a uniform amount of herbicide across the entire field. Because weeds tend to grow in patches and re-occur in the same areas each growing season (Mortensen et al., 1995; Tang et al., 1999; Martin-Chefson et al., 1999), a uniform application of herbicide may not yield optimal results in terms of economic efficiency.

SSHM allows for selective herbicide application based on zones of weed density and may result in a 30-72% reduction in herbicide requirements (Mortensen et al., 1995), thus increasing production profitability (Medlin et al., 2000). With reported Canadian pest control product sales totalling $1.34 billion (78% of which were herbicide) in 2005 (Crop Life, 2007), more efficient weed control practices could constitute a substantial savings to producers. Secondarily, SSHM techniques also reduce environmental contamination potential, in terms of leaching to groundwater and losses to the atmosphere (Lindquist et al., 1998; Lippert and Wolak, 1999; Smith and Blackshaw, 2003).

Effective implementation of SSHM techniques requires detailed spatial information on the location and population density of weed species at the field scale. This information is costly and time consuming when acquired through traditional field survey techniques. Advances in spatial information technologies, including Global Positioning Systems (GPS), Geographic Information Systems (GIS) and Remote Sensing (RS) are offering land managers new tools for locating and targeting weed infestations (Swinton, 2005).

Passive optical remote sensing technology, which samples the reflected solar electromagnetic (EM) radiation over a specific area or picture element (pixel), provides information about targets of interest (ie. weed and crop species) from which reflectance features and spatial objects can be extracted. Differences in these measured characteristics can then be used to create generalized classes (classification) over agricultural fields. Investigations into the use of RS image data (ground-based, airborne and satellite) for the detection and mapping of weed infestations have provided

encouraging results (Tian et al., 1999; Bechdol et al., 2000; Tang et al., 2000; Radhkrishnan et al., 2002), as reviewed in Chapter 2.

SSHM systems can be separated into two main categories based on how the RS data are acquired and processed. The first is a system where a weed map is produced from satellite or airborne RS data acquired prior to herbicide application. A GIS integrated with the sprayer would then selectively activate the spray nozzles based on the prescribed map locations. This technique would allow not only weed location and density to be used, but additional information including past yield, soil type and organic matter content could also be integrated into making the spray decision (Brown and Steckler, 1995). The main limitations to this type of system are the timely acquisition of image data and associated cost of tasking airborne and satellite missions.

These limitations can be mitigated through integration of the sensor, processing system and sprayer on the same implement in the field, which can then operate in real-time. As a producer navigates the field, the onboard sensor would acquire image data, process these data into weed location/density information and a resulting weed prescription map would be interpreted with the herbicide being applied "on the fly" only in required areas. The very high spatial resolution of image data acquired (mm scale) at ground level increases potential to detect not only spectral differences between weed and crop species but also spatial differences in leaf shape and orientation. Challenges to this type of system include computational load of onboard processing and the requirement for efficient and accurate implementation of automated weed detection procedures (Tang et al., 1999).

This study investigated the image acquisition and processing component for a real-time SSHM system, and developed a procedure for the detection of select weed species in crops during the optimal herbicide application timeframe. A prototype camera system was used to acquire very high spatial (mm scale) and spectral (10 nm wavebands) image data over weed and crop treatments in both laboratory and field-based trials. The spectral and spatial resolution of image data acquired enabled testing the capability of both leaf shape and reflectance characteristics for discrimination of crop and weed species. Two classification techniques were evaluated for species discrimination: Artificial Neural Networks (ANNs) and Maximum Likelihood Classification (MLC). This initial detection step is required for subsequent mapping of weed location and prescribed locations for herbicide application.

Research objectives were to:

(a) evaluate the potential of very high spatial resolution image data for segmentation of individual leaves and separation of background (soil, litter) from vegetation,

(b) identify the spectral characteristics from lab and field-based image data for use in weed/crop differentiation,

(c) evaluate two supervised classification techniques (MLC and ANN) for accuracy in species recognition and determine if a full hyperspectral dataset is required or a reduced number of bands are sufficient in classifying these data and

(d) characterize the effect of plant stage on spectral reflectance characteristics, and if this variability can be accounted for in the classification procedures developed.

Investigation into spectral and spatial differentiation of weed and crop species is required for development of SSHM techniques which are practical to the agricultural producer. The following chapter reviews the state of the art with respect to species discrimination using spectral and spatial characteristics and the use of image processing

techniques including segmentation and pixel-based classifiers for identification of weed/crop species, a preliminary step in the production of herbicide prescription maps.

CHAPTER 2 LITERATURE REVIEW

2.1 Introduction

Implementation of SSHM techniques requires knowledge of the location and density of weed species to make subsequent herbicide application decisions. This chapter identifies the spectral and spatial characteristics which have been used in discrimination of plant species. Acquisition of RS image data and the image processing procedures used for defining these spectral and spatial characteristics are explained and examples of weed and crop discrimination, drawn from published literature, are presented.

2.2 Vegetation Species Differentiation

Characteristic feature differences must exist between vegetated species for accurate identification. The relationship of plant matter to incoming solar radiation is one feature which can be utilized to discriminate plant species. The plant tissue relationship to Electro-Magnetic (EM) radiation (reflectance and absorbance) is termed spectral signature, which is a measure of the reflectance properties of a target over a range of wavelengths (Figure 2.1).

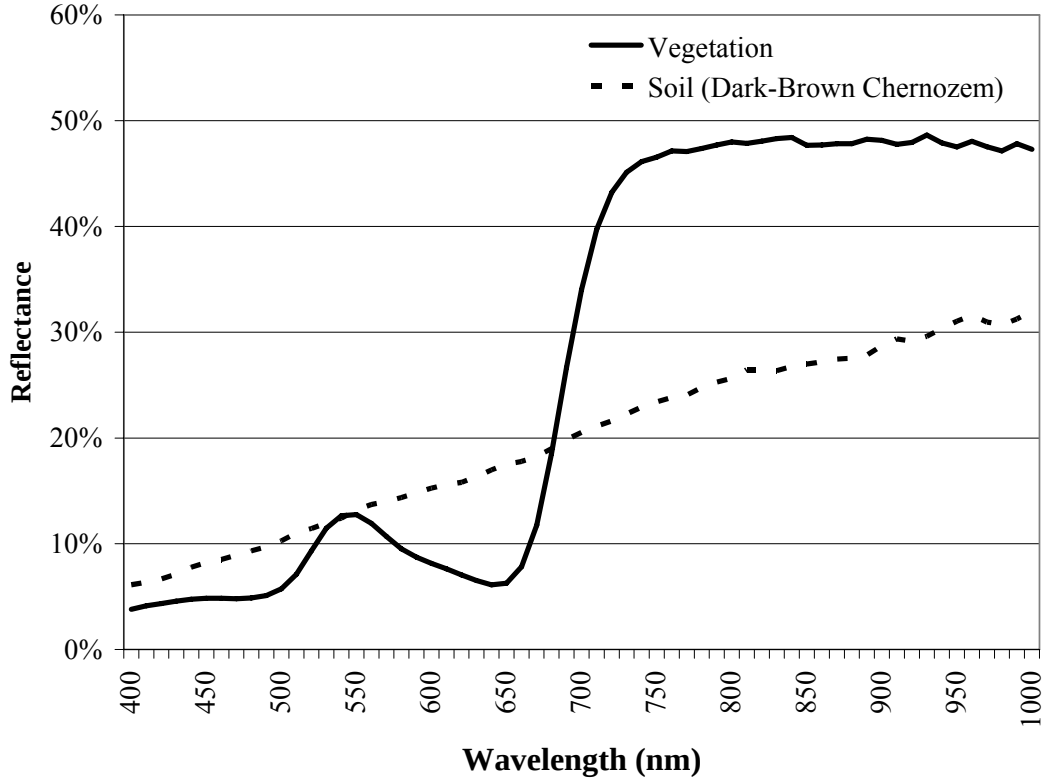

Figure 2.1 Typical reflectance curves for soil and vegetation from field data acquired July 19, 2005.

Spectral signatures of photosynthetic plant species are similar with several characteristic absorption features caused by photosynthetically active material and internal leaf structure. Absorption features occur in the spectral range of 400-2500 nm due to photosynthetic pigments (450 and 670 nm) and water (970, 1200, 1450, 1950 and 2400 nm) (Gausman et al., 1973; Lillesand and Keifer, 1987; Grant, 1987; Curran, 1989; Vrindts et al., 1999; Lamb, 2000). The magnitude of these spectral responses is a function of leaf thickness/structure, chlorophyll and other pigment concentrations and water content within the plant leaf (Lillisand and Keifer, 1987; Carter, 1991).

Chlorophyll and water content varies by plant species due to differences in physiology, and the ability to detect these variations using spectral response curves (signatures) is evident (Gausman et al., 1973; Lamb et al., 1999). This variability in spectral reflectance at specific wavelength regions of the EM spectrum, particularly in the visible and near-infrared (NIR), suggests potential for differentiation of weed from crop species (Zwiggelaar, 1998).

Use of not only spectral characteristics but also spatial characteristics such as leaf shape and structural differences may also be used to identify and discriminate plant species. For example, monocotyledon species characterized by long narrow grass-like leaves are very different from the broad and circular leaves in dicotyledons. Through investigation of leaf shape measurements (perimeter, area, roundness etc.), different plant species could be identified based on spatial characteristics.

Given these spectral and spatial characteristics identified as important for species discrimination, RS technology is a valuable resource as it can provide both spectral and spatial information of selected targets on the ground. The following section describes the process by which RS data are acquired and how information can be extracted and applied to plant species discrimination.

2.3 Information from Remote Sensing Techniques

RS is the process by which data are recorded about an object, area or phenomenon by a sensor that is not in direct contact with that object, area or phenomenon (Lillisand and Kiefer, 1987). In this study, RS refers to the measurement and subsequent recording of reflected EM radiation at wavelengths from the visible (400-700 nm) to near-infrared (700-1000 nm) regions as provided by the sensor system utilized. The spectral, spatial

and temporal resolution of the RS data are of particular importance as these resolutions have a significant effect on the processing methods used and the information that can be extracted.

Spectral resolution refers to the measurement width (wavelength) and number of wavebands recorded in the RS data. A multispectral dataset will contain less than 10 relatively wide (~60-100 nm) wavebands, while a hyperspectal dataset can have 200 or more narrow wavebands (~1-20 nm) and typically are contiguous (ie. uninterrupted across the measured spectrum). The spatial resolution or scale of RS data refers to the area that each picture element (pixel) in the image represents on the ground. This is a function of the system optics and the platform on which the sensor is situated. For a given sensor configuration, greater target to sensor distance results in a larger ground area represented by a single pixel and therefore a lower spatial resolution. Generally, a sensor placed on a satellite platform will have lower spatial resolution than an airborne system, with the highest spatial resolution (mm scale) obtained using ground-based systems. Temporal resolution is simply the number of RS data acquisitions over time.

Data processing techniques are used to derive information about objects and areas of interest from the RS data. These processing tasks used in characterizing spectral and spatial differences, particularly in relation to weed and crop species discrimination are described in the following sections.

2.3.1 Spatial Characteristics

The very high spatial resolution of ground-based sensors provides an opportunity for species discrimination based on leaf shape and textural features (Rosin, 2003; Cho et al., 2002). The majority of past studies utilized multispectral colour (Red, Green, Blue)

(RGB) charge-coupled device (CCD) sensor systems, as access to hyperspectral systems was limited. Defining leaf shape requires identification of foreground regions (plant pixels) and elimination of background features (soil and litter pixels) (Martin-Chefson et al., 1999). Foreground vegetation pixels can then be isolated using threshold techniques. Alternatively, processing methods such as watershed segmentation exist for identification of not only plant pixels but defining individual plant leaf segments.

2.3.1.1 Image Thresholding

Thresholding is a common image processing technique to generalize image data and segment objects of interest based on the magnitude of spectral response. This procedure involves selection of the upper and lower range of pixel values for the object of interest (foreground pixels) and assigning them a single value, segmenting the image data into two classes, foreground and background. A transformation of RGB image data to Hue, Saturation and Intensity (HSI) colour space is a common practice to alleviate the effects of variable illumination (Cheng et al., 2001; Burks et al., 2000a) and typically provides better segmentation results.

Tang et al. (2000) reported a method for segmenting plant matter from background using a genetic algorithm based on HSI. The genetic algorithm is an adaptive search method modelled after the genetic evolutionary process. The algorithm searched for the best three-dimensional threshold boundaries in HSI colour space, which represented foreground (plant matter) in an image. This family of algorithms was highly efficient in search problems and was rarely affected by local minima due to the parallel exploration of the search space. The study utilized a colour CCD camera (Sony XC-003) to obtain imagery of soybean (*Glycine max* (L.) Merr.) under variable illumination

conditions. Similar results were obtained between algorithm output and manually segmented images and the authors suggested this method could be used as a first step in a weed detection procedure to account for variable illumination conditions.

Another proposed method for recognizing plant species included both spectral and leaf geometric features used in a classification scheme (Chapron et al., 1999). Imagery obtained over corn (*Zea mays* L.) and weed plots using a four band (RGB and NIR) CCD camera (bandwidths and model not reported) were segmented into green plant matter and soil background using a series of Legendre filters (to remove signal noise) and thresholds of colour transformations. Colour transformations included HSI, and the Commission International de l'Eclairage colour space developed for perceptual uniformity (Cheng et al., 2001). The resulting image was classified into two classes (corn, not corn) using an expert system involving morphological filters that identified leaf shape. The procedure was robust under different illumination conditions but leaf overlap in the imagery hindered the classification accuracy, as the model could not efficiently separate overlapping leaves.

The calculation of texture statistics from HSI colour space has also shown promise in discrimination of weed species. Burks et al. (2000b) used an image analysis technique based on a Colour Co-occurrence Method (CCM) to discriminate five greenhouse grown weed species [large crabgrass (*Digitaria sanguinalis* Scop.), giant foxtail (*Setaria faberi* Herrm.), common lambsquarters (*Chenopodium album* L.), ivyleaf morning-glory (*Ipomoea hederacea* (L.) Jacq.), velvetleaf (*Abutilion theophrasti* Medicus)] and soil. The method involved colour transformation of RGB imagery (acquired with a colour CCD JVC TK-870U camera system) to HSI co-ordinates

followed by CCM matrix generation on the HSI bands, and Discriminant Analysis (DA) classification. To reduce the dimensionality of the CCM texture statistics (33 for each of the HSI matrices) and select layers that best identified textural differences between species, the authors used a Stepwise Discriminant Analysis (SDA). Overall classification accuracy was 93% for all six ground cover classes using 11 CCM texture features. The selected texture features used in the classification scheme did not include the intensity component thus reducing the processing time by one third and offering greater potential for a real-time herbicide application system.

2.3.1.2 Watershed Segmentation

Watershed segmentation is a technique for identifying plant leaf segments within image data. Once defined, leaf shape differences can be used for species discrimination. This technique considers a grey scale image as a topographic surface with pixel values as "elevations". Low points or minima on the surface are identified and the surface is flooded from these points. Building a "dam" keeps water from flowing between basins as flooded areas meet. Once the surface is completely flooded, watershed lines represented by dams define regions in the image (Vincent and Soille, 1991; Beucher, 1992; Bleau and Leon, 2000; Rambabu et al., 2004).

Since its introduction by Beucher and Lantuejoul (1979), many researchers have published alterations to the algorithm to improve efficiency. The method developed by Vincent and Soille (1991) significantly reduced computational requirements for segmentation and has made watershed segmentation an operational tool for practical use (Li et al., 1999). Though watershed segmentation has not been applied to leaf object

identification, it has been utilized to segment plant pixels from background (soil) in colour image data (Soille, 2000) using the red-green feature space.

2.3.1.3 Leaf Shape Extraction

Once plant pixels are identified within the image through thresholding or other segmentation procedures, leaf shape measurements can be extracted. These can include, but are not restricted to, measurements of perimeter, area, aspect, roundness, compactness and elongation (Cho et al., 2002). Aitkenhead et al. (2003) obtained overall classification accuracies of 62 to 67% in the identification of ryegrass (*Lolium perenne* L.) and fat hen (*Chenopodium album* L.) in Autumn King carrot (*Daucus carota* L.) crops through a single shape measurement (perimeter^2/area). Using three shape features (perimeter/broadness, elongation and aspect ratio) produced class accuracies of 92% for radish (*Raphanus sativus* L.) and 98% for an amalgamated weed class [purslane (*Portulaca oleracea* L.), crabgrass and goosefoot (*Chenopodium album* L.)] (Cho et al., 2002). Limitations to segmentation procedures for discrimination of crops and weeds based on leaf shape characteristics include size/stage of plant, leaf occlusion and shadow effects (Chapron et al., 1999; Brown and Noble, 2005).

2.3.2 Spectral Characteristics

RS data can be used to derive information about the spectral characteristics of vegetated species. Classification is an image processing technique used to generalize complex image data into more meaningful categories or classes based on similarities in spectral pixel values. Different methods exist including statistical classifiers that group pixels based on clusters formed in the spectral domain. Artificial intelligence methods

such as ANNs, which attempt to model biological neural function, have been used in image classification and are shown to provide accurate and computationally efficient results (Atkinson and Tatnall, 1997). Studies involving the detection of weeds in agricultural cropping systems using pixel-based classification techniques are abundant (reviews by Lamb and Brown, 2001; Noble et al., 2002), and can be applied to RS image data of any spatial and/or spectral resolution. The following sections review statistical classifiers for detection of weeds in agricultural crops, followed by application of ANNs to crop/weed discrimination.

2.3.3 Statistical Classifiers

2.3.3.1 Airborne Sensing

Research into the creation of weed maps at the field scale using multi- and hyperspectral airborne remote sensing systems has been an active field of study (Brown et al., 1997; Lamb and Weedon, 1998; Medlin et al., 2000). Though limitations exist for spatial resolution, these systems are well suited to large area mapping and can provide information on weed location at the field level but not at the individual plant level.

Lamb and Weedon (1998) mapped panicgrass (*Panicum effusum* R. Br.) in canola (*Brassica napus* L.) stubble using MLC and Normalized Difference Vegetation Index (NDVI) thresholding. A four band CCD airborne system acquired spectral information over the blue (440 nm), green (550 nm), red (650 nm) and near-infrared (770 nm) regions of the electromagnetic spectrum at a spatial resolution of 1 m. The separation of green plant matter from soil and stubble background resulted in an overall classification accuracy of >87% for both MLC and NDVI threshold methods. Brown and Steckler (1995) also attempted to classify four weed species (green foxtail (*Setaria viridis* (L.)

Beauv.), quackgrass (*Agropyron repens* (L.) Beauv.), dandelion (*Taraxacum officinale* Weber) and lambsquarters in two no-till corn fields using MLC on both colour and colour-infrared photography (10 cm spatial resolution). Confusion between dandelion and lambsquarters was observed and these two classes were grouped. Species differentiation was obtained in this study with an overall accuracy of 75%.

Medlin et al. (2000) used a four band CCD airborne system with one green (535-545 nm), two red (690-700 nm and 715-725 nm) and a NIR (835-845 nm) band, to acquire data over two early season (eight weeks post-seeding) soybean fields. The spectral response was linked to ground-based density populations of three weed species [pitted morning-glory (*Ipomoea lacunose* L.), sicklepod (*Senna obtusifolia* (L.) Irwin & Barnaby) and horsenettle (*Solanum carolinense* L.)]. The relationship between the spectral response and weed density was tested through SDA. The imagery was classified using DA for the presence or absence of weeds rather than each weed species. A positive relationship between weed density and classification accuracy was established but differentiation of weed species was not successful.

Few studies have tested the potential for species discrimination and weed map production using high spectral resolution airborne hyperspectral image data. Bechdol et al., (2000) acquired hyperspectral data using the Airborne Imaging Spectroradiometer for Applications system (SPECIM, Oulu, Finland), which records data over the spectral range of 450 to 900 nm. Images of three spatial resolutions (1, 2 and 3 m) were acquired over corn and soybean fields infested with eight weed species. The imagery was atmospherically corrected and converted to reflectance. Through classification of minimum noise fraction feature space, weed infestation zones showed agreement with

ground-data collected over all spatial resolutions. Discrimination amongst weed species was not achieved.

2.3.3.2 Ground-Based Sensing

Ground-based sensing platforms offer many advantages over airborne or satellite systems. These include absence of atmospheric scattering/absorption and very fine spatial resolution as the target is situated closer to the sensing system. A major limitation is spatial coverage, but in precision agricultural techniques aimed at individual fields, data are not required for large areas. Several methods have been developed for weed detection using statistical classifiers at ground level, using both multi- and hyperspectral image data.

An inexpensive CCD camera (Canon model 760) was utilized by Brown and Steckler (1993) to collect spectra (440, 530, 650, 730 nm) over a no-till corn field with two weed species [quackgrass and milkweed (*Asclepias syriaca* L.)]. Image data were acquired at 8 m as well as 600 m (aerial) above the target resulting in spatial resolutions of 15 and 150 mm respectively. Using MLC, >80% overall accuracy was obtained with the 600 m acquisition when defining three classes (weeds, corn and background) though individual weed species could not be differentiated. The 8 m acquisition enabled separation of individual species as 66% of corn, 90% of quackgrass and 100% of milkweed pixels were correctly classified. A similar project was reported (Brown et al., 1994) using the same sensing system and imaging techniques to acquire data over no-till corn with seven weed species. Again, MLC was used with optimal results obtained when weed species were joined into a single class.

Because many weeds can be characterised by red stems, El-Faki et al. (2000a, b) attempted to differentiate crop and weed species based on stem colour. Off nadir image data (45° incident angle) were collected using a colour CCD video camera (Sony XC-711) and provided a detailed view (mm spatial resolution) of the plant stems. Imagery was collected over trays of plants grown in a greenhouse. Trays included hard red winter wheat infested with wild buckwheat (*Polygonum convolvulus* L.), cheat grass (*Bromus secalinus* L.) and field bindweed (*Convolvulus arvensis* L.) as well as soybean infested with johnsongrass (*Sorghum halepense* (L.) Pers.), redroot pigweed (*Amaranthus retroflexus* L.) and yellow foxtail (*Setaria glauca* (L.) Beauv.). The method involved testing both DA and ANNs for classification. A pre-processing step masked plant leaves, with the remaining stems passed to the classifications (DA, ANN). Mis-classification rates for most weed species were below 3% for both methods, with the DA producing the highest accuracy in crop classification (least square means of 55% for soybean and 62% for wheat). The authors stated that crop and weed stage were factors affecting the accuracy of weed detection.

Though ground-based hyperspectral imaging systems are rare, spectroradiometers which acquire spectral response of a single area (similar to a single pixel) provide the opportunity to measure reflectance characteristics of crop and weed species at very high spectral resolution and have provided encouraging results in weed detection and species discrimination studies. Vrindts et al. (2002) used an optical spectrum analyzer (Macam Photometrics Ltd., Livingston, Scotland) to obtain lab spectra from 400-2000 nm of seven weed species as well as corn and soybean. Through SDA, band ratios were selected that were deemed best for species discrimination. DA of these band ratios

produced classifications in which 97% of the weed and crop lab spectra were correctly classified. In the field, spectra from 400-900 nm were obtained using an Imspector V9 spectrograph (SPECIM). Using the same DA method, 90% of the crop and weed spectra were correctly classified. Illumination was a limitation as the discriminant models were developed under specific light conditions.

DA classification provided good results in a study of excised leaves of two crop (canola and spring wheat) and five weed species (lambsquarters, green foxtail, redroot pigweed, wild mustard (*Sinapis arvensis* L.) and wild oat (*Avena fatua* L.)) (Smith and Blackshaw, 2003). An ASD fieldspec pro spectroradiometer (Analytical Spectral Devices Inc., Boulder, CO.) and an LI-1800 integrating sphere (Li-COR Inc., Lincoln, Nebraska) were used to obtain spectra. Spectral resolution of these data were resampled to hyperspectral (350-2500 nm at 10 nm intervals) and multispectral (representing the Landsat wavebands) datasets. Species classification accuracies of 89% and 90% were obtained using the multispectral and hyperspectral datasets, respectively. The authors suggested that the hyperspectral dataset was optimal as confusion was only observed within the monocotyledon species, whereas confusion between monocotyledon and dicotyledon species sometimes occurred in classification of the multispectral dataset.

An imaging spectrometer used by Borregaard et al. (2000) provided data for an extensive study of weed discrimination techniques including linear and quadratic DA, Principal Component Analysis (PCA) and partial least-squares regression. Using both visible (400-700 nm) and NIR (660-1060 nm) line imaging spectrometers (VTT Electronics, Oulu, Finland), spectral data were acquired for two crops [sugar beet (*Beta vulgaris* L.) and potato (*Solanum tuberosum* L.)] and three weed species (fat hen,

bindweed and fools parsley (*Aethusa cynapium* L.). The imagery was segmented to obtain pure plant spectra used in classification method evaluations. The bi-linear methods proved to be the most efficient with overall accuracies of 70-80% on four species (one crop and three weeds), and 90% when aggregated into two classes (crop and weed).

2.3.4 Artificial Neural Networks

With the advancement of computing capability and the substantial amount of data supplied by imaging sensors, there is an increasing need for efficient data processing and interpretation tools. Artificial neural networks, which attempt to model biological neural pathways, have been used extensively in many different applications. The acceptance of ANNs in the field of remote sensing is due to several factors including the ability to handle complex feature space, to be computationally efficient and, to integrate different types of data (Atkinson and Tatnall, 1997). ANNs are also advantageous in that they can handle classes with two or more clusters in spectral space (i.e. aggregated class "soil" which contains both "bare soil" and "crop litter" pixels) and as a non-parametric approach, they do not have underlying assumptions such as multivariate Gaussian normality (as in MLC). For classification of plant reflectance spectra, which are typically not normally distributed (Noble and Crowe, 2005), ANNs may present an advantage over more traditional techniques.

ANN development began with the introduction of the perceptron (Rosenblatt, 1958), a very simple feed-forward network model used to solve linear problems. Network models were incapable of distinguishing classes that were not linearly separable until the mid-1980's with the development of back-propagation training (Smith, 1993).

Through the past 40+ years, advancement in network architecture, training methodology and software design have resulted in the introduction of many ANN types, the most common being the feed-forward Multi-Layer Perceptron (MLP) trained by the back-propagation algorithm (Atkinson and Tatnall, 1997; Kannellopoulos and Wilkinson, 1997).

The MLP network consists of three or more layers including an input layer, one or more hidden layers and an output layer (Figure 2.2). Each layer contains a number of nodes which model biological neurons assembled by weighted channels creating a network. Input values are passed to the hidden layer with associated weights assigned to the connecting pathways. In each neuron, the weighted sum of all pathways is calculated and a non-linear (typically "sigmoid") transformation function is applied to model non-linear transfer effects. The value then passes to the output layer (or subsequent hidden layer(s)). The output layer can have one or more nodes, with values ranging from 0-1. Each class is assigned a specific output range, and the output value is classified accordingly.

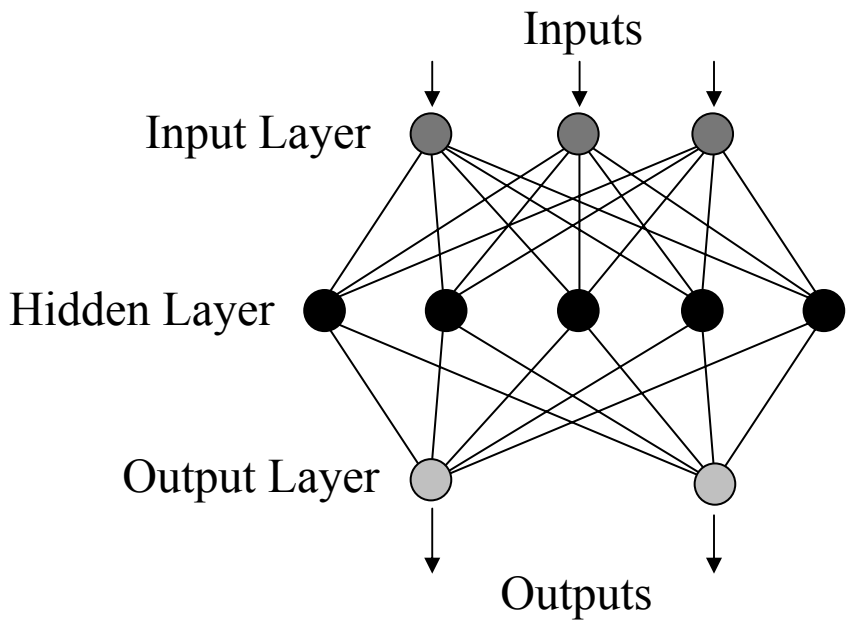

Figure 2.2 The Multi-Layer Perceptron (MLP) network architecture.

Training the feed-forward MLP network is commonly achieved through back-propagation. This supervised training method utilizes input and output pairs to compute an overall error for the entire network. This overall error is minimized through an error signal that is fed back through the network and alters the individual connection weights (Lawrence, 1994). By utilizing known input and output pairs, the weights are adjusted through several iterations (termed epochs) until the appropriate output is achieved and overall network error is minimized.

One issue with ANN use is that it can be difficult to build the network model properly to achieve optimal or near-optimal network architecture, especially given the number of input parameters involved. This complexity has been somewhat mitigated with the release of commercial neural network software packages that provide initial values for network specification although these values are highly dependent on the application.

Neural networks first appeared in the remote sensing literature in the late 1980's (Key et al., 1989; Benediktsson et al., 1990), with application to weed-crop discrimination appearing in the late 1990's (Yang et al., 1998, 2000; Moshou et al., 2001). Ground-based imaging sensors present the classifier with vast amounts of target information in the spatial and/or spectral domains to which ANNs are particularly well suited. This is important in real-time image processing systems that require computational efficiency. The following section reviews several studies in which ANNs were utilized for classification of weed species in agricultural cropping systems.

2.3.5 ANN Classification of Weeds in Agriculture

Machine vision based weed detection techniques provide very high resolution spatial imagery but are lacking in spectral dimensionality. In these applications, shape characteristics of plant leaves are investigated for discriminating species, particularly broadleaf (dicotyledon) crops infested with grassy (monocotyledon) weeds. Studies utilizing ANNs for classification of single plant image subsets, texture (co-occurrence measures) and leaf shape measurements aim to overcome the limited spectral information of machine vision sensors through incorporation of spatial species differences (Cho et al., 2002; Aitkenhead et al., 2003; Yang et al., 2000 & 2003; Burks et al., 2000a & 2005).

ANN classification of six weed species based on 11 CCM texture measurements (Burks et al., 2000b) expanded on a previous texture study (Burks et al., 2000a). The network architecture was evaluated by altering the number of nodes in the two hidden layers. The network model produced consistently high classification accuracies with the best topology producing a 97% overall (approx 90% individual class) accuracy.

Testing different network architectures based on classification accuracy also suggested that a large network does not necessarily produce the highest accuracies. This study was extended to evaluate different network types including counter-propagation, back-propagation, radial basis function and the DA classifier (Burks et al., 2005). The authors suggested the importance of reducing the number of input variables using SDA as a consistently successful procedure for simplification of the classification problem. From the several classification methods utilized, the back-propagation network model produced the highest accuracy (97%).

Cho et al. (2002) proposed an approach for discrimination between radish and three weed species based on leaf measurements (area, perimeter, length, width and length of major and minor axes) used to calculate eight shape features (aspect ratio, roundness, compactness, elongation, perimeter to broadness ratio, length to perimeter ratio, length to width ratio and cube of perimeter to area by length ratio) input to a MLP network model. Vegetation was segmented from the acquired colour imagery using Photoshop (Adobe Systems Inc., San Jose, CA), and shape characteristics were extracted using Image Pro Plus (Media Cybernetics Inc., Silver Spring, MD). SDA was used to identify three shape measurements (perimeter/broadness, aspect and elongation) classified using DA, while all eight measurements were used as input to an ANN. A network architecture of eight input, seven hidden and two output nodes classified 10 radish and 20 weed images with 100% accuracy, while the DA classifier produced 93% and 94% class accuracy in radish and weeds, respectively.

Aitkenhead et al. (2003) used a MLP neural network for discrimination amongst crop (carrot), weeds (ryegrass and fat hen) and soil. Image pre-processing involved

delineating subset blocks of 32 x 24 pixels that contained plant matter. Two image classification methods were tested. First, a shape characteristic (perimeter^2/area) mean was calculated from the training subset image data for the weed and crop classes and the validation blocks were classified based on distance to class means. Secondly, the image subsets identified were classified using an ANN with the whole image block passed to the input layer, two hidden layers and two output values (soil=0,0; carrot=1,0; weeds=0,1; crop and weeds=1,1). When plants of varied size were considered, the shape characteristic produced a classification accuracy of 62%, while the ANN classified between 62-82% of plant sample images correctly.

The effects of feed-forward back-propagation network architecture on classification of corn and seven weed species were evaluated in a study by Yang et al. (2000). Image data were collected using a Kodak DC50 RGB camera from which image subsets of 100 x 100 pixels containing a single crop or weed plant were manually selected. The subsets were converted from 24-bit colour to 8-bit grey scale. Several ANN architectures were created using Neural Network Toolbox v.2.0 for Matlab v.5.0 (Mathworks, Natick, MA) in which a single hidden layer contained 70 to 300 nodes with one (crop=1; weeds=0) or two nodes (crop=1,0; weeds=0,1) in the output layer. It was expected that the network with two output nodes would give an estimate of probability and that this would give some flexibility to interpretation of results. The single output network produced class accuracies of 70-100% for corn and 50-80% for weeds while the network with two outputs produced accuracies of 60-90% for corn and 40-80% for weed classes. McNemar and Briar Score statistics showed no significant differences between the various network models based on their predictive abilities. This suggested the

simplest model (least hidden and output nodes) was as effective in crop/weed discrimination as the more complex model.

This study was later expanded to detect four weed species in corn (Yang et al., 2003). Subset images of single plants were again defined (60 x 60 pixels) and converted to grey scale with four orientations per image (0°, 90°, 180° and 270°). Two types (crop/amalgamated weed and crop/single weed) of ANNs were developed using NeuralWorks Professional II v5.23 (NeuralWare Inc., Pittsburgh, PA) with a single hidden layer of multiple nodes (100 – 1000) and one and two output nodes. The resulting networks produced accuracies of 54-90% for corn and 32-100% for single weed species. This performance range indicated the importance of sample size and network architecture. Species type also affected classification accuracy as the worst classification accuracy was for corn and quackgrass, both of which are monocotyledon species and have similar leaf structural characteristics. Higher class accuracies were obtained for the crop/individual weed as opposed to the crop/amalgamated weed class.

Discrimination between sunflower (*Helianthus annuus* L.), common cocklebur (*Xanthium strumarium* L.) and background using three band (RGB) ground-based image classification with a MLP network using 1, 2 and 3 hidden layers was recently conducted (Kavdir, 2004). Network models developed consisted of sunflower-weed, plant-bare soil and sunflower-weed-soil classification schemes. The architectures consisted of 4800 inputs (3 colour values x 40 x 40 pixels) with 35-300 nodes in the first, 15-100 in the second and 7-15 in the third hidden layers.

The best classification for sunflower-weed scheme was obtained using three hidden layers (50 x 25 x 7) with 70 of 86 images correctly identified. Models with one or

two hidden layer architectures achieved slightly lower accuracies, though logistic regression showed no statistically significant difference in networks with 1, 2 or 3 hidden layers in discriminating plant and soil. Classification of the sunflower-weed-soil scheme had 93 of 129 images correct with one hidden layer and 103 of 129 using models with two hidden layers. Again classification accuracy of the ANN models was highly sensitive to network architecture. Because shadow and variability in plant size were inherent in these image data the author suggested further work should focus on in-field experiments where soil type and crop residue may affect classification accuracies.

Few studies have addressed weed-crop discrimination with ANNs using ground-based hyperspectral data. As discussed in section 2.1, plant spectral reflectance characteristics in bands outside the visible region of the electromagnetic spectrum provide more information than RGB colour imaging sensors and may increase the feasibility of weed-crop discrimination. Moshou et al. (2001) collected point spectra (200-2000 nm at 10 nm wavelengths) over corn, sugar beet and several weed species (individual species not identified). Discriminatory bands were selected from the 200 available using correlations between the two classes (high correlation indicates more information content contained within the band).

This procedure identified five bands for corn-weed and three bands for sugar beet-weed classifications. Different ANN types were tested including MLP trained using adaptive learning rate and momentum, Self-Organizing Map (SOM) trained with local linear mappings and, probability neural networks. The MLP classifier accuracies were 90% / 66% (corn / weed) and 86% / 94% (sugar beet/weed) but the best performance was observed in the SOM network with class accuracies of 96% / 90% (corn / weed) and 98%

/ 97% (sugar beet / weed). The authors suggested that the SOM network obtained faster convergence and produced better overall classification performance.

2.4 Summary

Research into the detection and discrimination of weeds in crops from both ground-based and aerial platform remote sensing systems is extensive. Spectral, spatial and temporal resolution often limits using aerial and satellite platform sensors for plant species discrimination and revisit schedules of satellite-based systems can hinder acquisition of data at critical plant stages (Radhkrishnan et al., 2002). Ground-based sensor systems are an attractive alternative due to the very high spatial resolution (mm scale) of image data but attention must be given to the increased computational cost of processing these data (Brown and Noble, 2005). Few studies have investigated the potential of hyperspectral image data for weed crop discrimination mainly due to lack of sensor system availability and higher cost.

Segmentation techniques, especially thresholding have consistently been applied for separation of foreground vegetation pixels from background in very high spatial resolution image data. This first step of segmentation can be used to define shape characteristics and also identify foreground pixels in RS image data. Identification of vegetation pixels can simplify the weed-crop classification problem through eliminating the need for soil or litter classes.

Building on past research, this study investigated the potential for weed and crop discrimination from the rich information (spectral and spatial) ground-based hyperspectral image data can provide. The following chapter reviews equipment and

methods used in acquisition and analysis of RS data for addressing the study objectives introduced in Chapter 1.

CHAPTER 3 MATERIALS AND METHODS

3.1 Introduction

This chapter describes equipment and procedures used in acquisition of hyperspectral image data and its evaluation for detection of selected weed species in post-emergent crops. This is followed by radiometric correction and procedures for conversion of raw image data to reflectance. The laboratory and field experimental design is presented followed by image segmentation techniques explored for identifying pixels of vegetation as well as identification of individual leaves within acquired image data. A method for selection of a subset of wavelengths, which are important for species discrimination, is presented as well as classification (MLC and ANN) techniques used to define species location within the image data. Validation methods for assessing classification accuracy, important for comparison of the two classification procedures, are then explained.

3.2 Hyperspectral Imaging System

The hyperspectral imaging system (Figure 3.1) and image acquisition software were developed by DeltaTee Enterprises Ltd. located in Calgary, Alberta, Canada. The system uses a magnetic carriage to "step" a linear variable filter (Schott Veril, VIS-NIR 200) across a charge-coupled device (CCD) sensor for hyperspectral image acquisition. The interference filter's central wavelength varies linearly over a 200 mm length of glass substrate (Figure 3.2) and permits acquisition of a data cube with 61 wavebands from 400 – 1000 nm at 10 nm increments. The imaging sensor, manufactured by Point Grey Research (Vancouver, British Columbia) uses a 0.5 inch progressive scan CCD sensor

(Sony, ICX414AL). This sensor outputs a 640 x 480 pixel image with a signal to noise ratio of greater than 60 dB. Image data output are 16-bit unsigned integers, enabling a raw digital number (DN) dynamic range of 0 – 65535. The system focuses incoming radiation with an 8 mm C-mount VIS-NIR lens (Schneider Kreuznach, Germany) fixed to create 44 º vertical and 33º horizontal fields-of-view with the focus and aperture (f/1.4 to f/11) adjusted manually. This range in aperture settings ensures the system can be set to avoid saturation (DN reading above the 65535 limit of the CCD).

The image acquisition software (SPDaq, DeltaTee Enterprises Ltd.) allows electronic shutter and waveband width adjustments, and was used to acquire, save and perform radiometric correction of the hyperspectral image data.

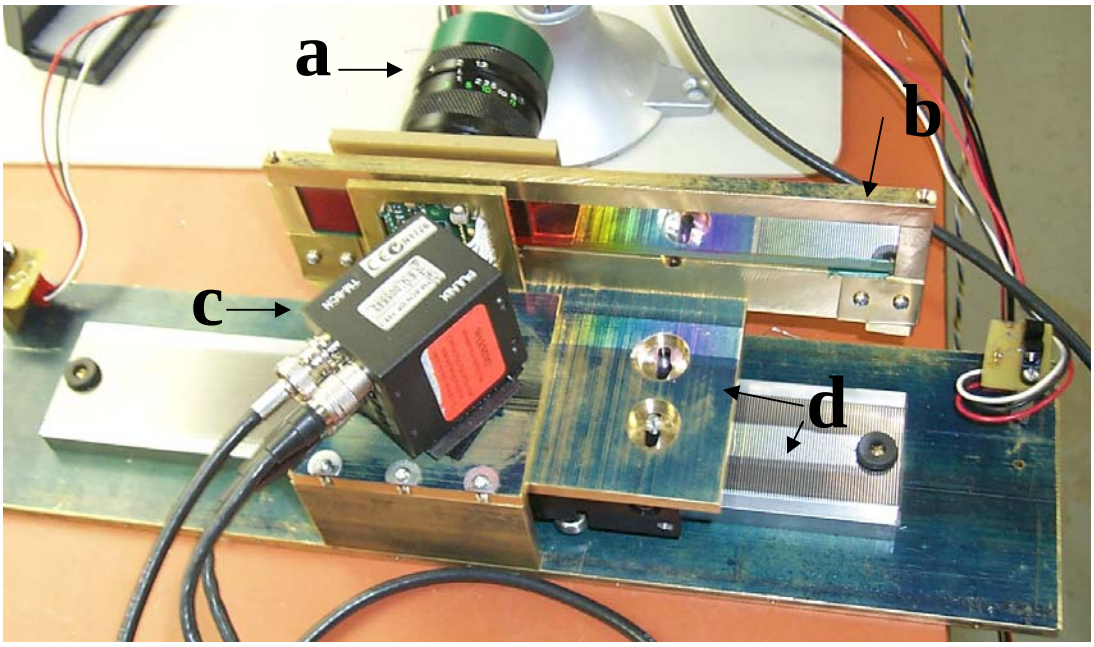

Figure 3.1 Hyperspectral imaging system components; a) lens, b) linear variable filter, c) imaging sensor and d) carriage system.

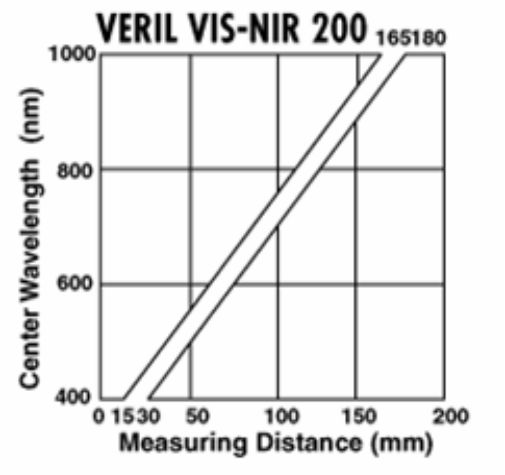

Figure 3.2 Linear relationship between measuring distance and wavelength in 200 mm filter (obtained from Edmund Optics, 2007).

3.3 Calibration of Image Data

Prior to image analysis, the acquired image data were radiometrically corrected. This consisted of three steps; dark correction, frequency resampling and uniformity correction. The final processing step, conversion to reflectance, was achieved using the ENVI/IDL software package (ITT Industries Inc., Boulder, CO). The following sub-sections discuss each correction applied.

3.3.1 Dark Current Correction

Dark current correction accounts for internal signal noise and false response in the CCD potential wells inherent to this type of imaging system. Thermal energy read as incoming photons can constitute a false reading of incoming radiation termed dark noise. Dark noise is positively related to thermal energy, and as the temperature of the imaging environment changes, particular attention must be given to dark noise effects. Correction involved collection of 200 frames with the lens covered to eliminate all sources of incoming radiation. The mean DN (n=200) for each pixel was calculated creating an

image of measured dark noise which was subtracted from each band in successive image acquisitions. Dark noise correction data were acquired regularly throughout the period of image data collection to account for variation in dark noise effects.

3.3.2 Frequency Resampling

The raw image data consisted of several frames in which wavelength varied across the X dimension due to the linear variable filter used in the hyperspectral image acquisition. A frequency resampling technique applied to the data cube transformed these data into frames of one consistent wavelength. The procedure shifts the frequency data through a linear interpolation to adjacent images to produce a single wavelength horizontally across the image (Figure 3.3). A number of extra images are taken to avoid extrapolation. The factors for this correction (slope and intercept) are specific to the filter used in the imaging system and were calculated by the manufacturer.

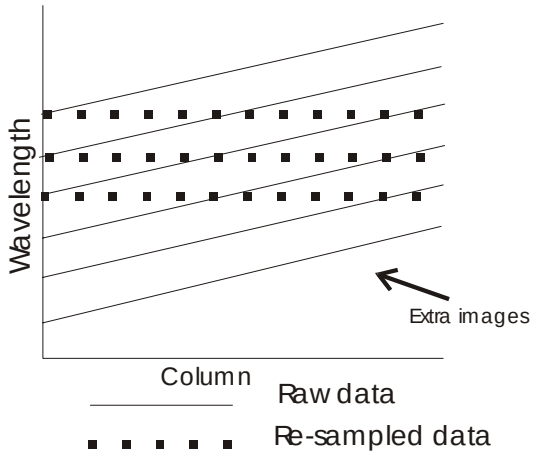

Figure 3.3 Example of frequency resampling applied to image data cube.

3.3.3 Uniformity Correction

Uniformity or flat field correction reduces variability in the imaging scene caused by fluctuation of the quantum efficiency of each potential well in the CCD matrix, termed photo response non-uniformity. Secondly, as a result of circular lens optics, a gradient effect (viginetting) across the image is inherent in any imaging system. Uniformity correction, which corrects these effects, can be calculated by filling the field-of-view with a target of consistent reflectance. An integrating sphere was developed and used for uniformity coefficient collection at DeltaTee's laboratories.

The camera was setup to view the evenly illuminated integrating sphere. For each f/stop the shutter speed was adjusted so that the maximum value in the dataset was approximately 75% of the full dynamic range. With the optimal shutter speed established, a full hyperspectral data cube was acquired and dark correction applied. The wavelength at which the highest signal response occurred was identified, and the average value was calculated for that band. A correction coefficient matrix was created by dividing the average value by the value for each pixel (Equation 3.1). Multiplication of this uniformity coefficient matrix with each band in the acquired hyperspectral data produces a uniformity corrected image. The coefficient matrix is calculated by:

$$C_{x,y} = Avg / U_{x,y} \tag{3.1}$$

where Avg is the average DN value, $U_{x,y}$ is the DN value of a pixel at column x and row y, and $C_{x,y}$ is the correction coefficient for the pixel at column x and row y.

3.3.4 Reflectance Conversion

The final step of image processing involved conversion of DN values to reflectance. Reflectance is a measure of the percentage of incoming solar radiation reflected by an image target on a per pixel basis. This conversion required imaging a Spectralon (polytetrafluoroethylene) calibration panel. The panel reflects approximately 99% of incoming solar radiation across the 400-1000 nm wavelength range of the imaging system, with reflectance coefficients provided by the manufacturer (Labsphere, Inc., North Sutton, NH) at 50 nm increments (Appendix A).

Immediately before and after image acquisition, the Spectralon panel was imaged (f/11 and shutter speed = 2-4 ms) ensuring sensor saturation did not occur. The raw image pixel values of the reference panel were extracted and band means calculated. Acquisition of laboratory and field plot data required a slower shutter speed to provide appropriate signal strength to the CCD sensor, and typically ranged from 4-8 ms. The relationship between exposure time and DN output in the CCD sensor system evaluated and found to be linear up to the saturation point (DN=65535) (Figure 3.4). This suggested a conversion ratio could be applied prior to reflectance conversion, accounting for differences in shutter speed between the acquired panel and target image data.

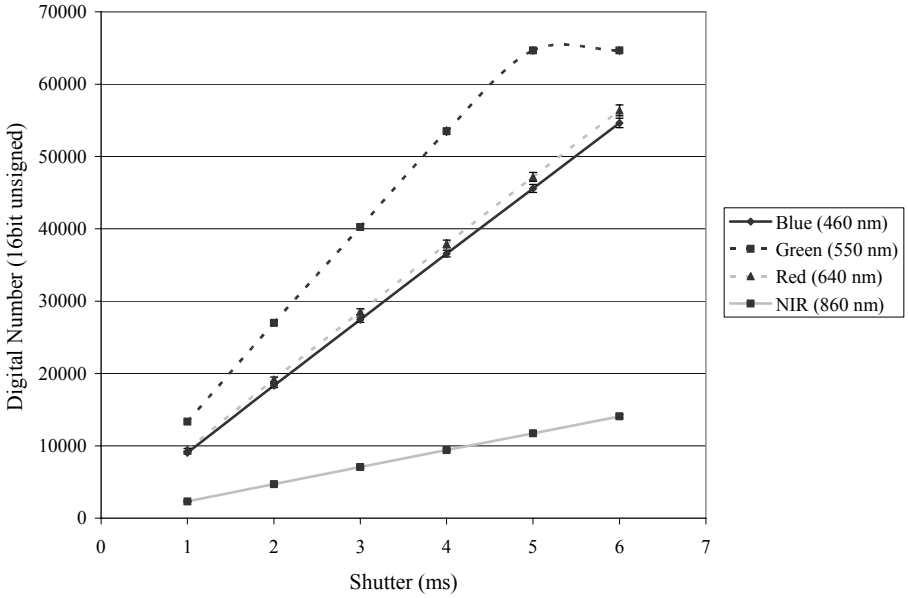

Figure 3.4 Relationship between electronic shutter and raw digital numbers on CCD sensor (Mean n=4544, error bars = +/- standard deviation).

An IDL program was written to convert the image data cubes to reflectance (Equation 3.2). The program includes an exposure multiplier (conversion ratio), which accounts for instances where the reference panel was collected at a different shutter speed (same aperture) than the target/plot images. For example, if a panel image acquired at 2 ms is used to correct a field image acquired at 6 ms then the exposure multiplier would be 3. The program multiplies the DN's of the calibration target by 3 before reflectance correction is run. Reflectance is calculated as:

$$R_{(x,y,b)} = (I_{(x,y,b)} * SP_{(b)}) / CT_{(b)} \quad (3.2)$$

where CT is the calibration target average DN, I is the image DN value, R is the image reflectance value, SP is the spectralon panel reflectance coefficient and x,y,b represent the horizontal coordinate, vertical coordinate and band, respectively.

3.4 Experimental Design

3.4.1 Crop and Weed Species

It was important that the weed/crop species selected in the study represent both monocotyledon and dicotyledon morphologies encountered in agricultural applications, as well as being of economic importance in western Canadian cropping systems. Based on these criteria, three crop species [Eclipse field pea (PEA) (*Pisum sativum* L.), Invigor 5020 canola (CAN) (*Brassica napus* L.), and AC Barrie spring wheat (WHT) (*Triticum aestivum* L.)] and two weed species [redroot pigweed (RRP) (*Amaranthus retroflexus* L.) and wild oat (WO) (*Avena fatua* L.)] were selected for investigation.

3.4.2 Laboratory Trial

Using laboratory and greenhouse facilities located at the Agriculture and Agri-Food Canada Research Centre in Lethbridge, Alberta, weed/crop mixtures were seeded in trays of Cornell mix, an equal-part mixture of sphagnum peat moss and vermiculite (Table 3.1). These treatments were grown in a greenhouse under sodium vapour lighting with a 16 hour day - 8 hour night cycle at a constant temperature of 21° C.

Table 3.1 Planting depth and seed placement for greenhouse reared crop and weed mixtures.

Species	Planting Depth (cm)	Seed Placement
canola	1.5-2	0.5 cm spacing
pea	5	0.5-1cm spacing
wheat	4	Seed end to end
redroot pigweed	Surface	Broadcast, and raked into surface
wild oat	1.5-2	Broadcast, covered with soil

Four replications of these treatments were planted at approximately two-week intervals. For this study, canola, redroot pigweed and a single wheat plant were transplanted into two trays. These trays provided a variety of leaf shapes and sizes, sufficient for initial testing of segmentation procedures.

3.4.3 Field Trial

The field study site was located at the Agriculture and Agri-Food Canada Research Centre in Lethbridge, Alberta (49.7°N, 112.833°W). The soil type was Dark Brown Chernozemic of lacustrine origin with a pH of 8.0 and 3% organic matter content. Weeds were surface broadcast on plots (5 m x 2.5 m) prior to seeding the various crops (Table 3.2). Seeder movement over plots allowed the broadcast weeds to be embedded in the soil, facilitating germination. During the seeding operation, nitrogen at 40 kg ha^{-1} and phosphorous at 10 kg ha^{-1} were banded 10 cm deep between crop rows.

Table 3.2 Seeding procedures for the field trials.

Species	**Rate**	**Depth (cm)**	**Row Spacing (cm)**
canola	8 kg ha^{-1}	1-2	23
pea	253 kg ha^{-1}	5	23
wheat	124 kg ha^{-1}	4	23
redroot pigweed	27 g $plot^{-1}$	Surface	N/A
wild oat	100 g $plot^{-1}$	Surface	N/A

Field plots of the eleven treatments (5 monocultures and 6 weed/crop combinations) (Table 3.3) were seeded on four dates (Table 3.4) to increase the window of opportunity for collecting timely (weather/crop stage) image data. Spring flooding hindered the first two seeding dates but hand watering of trial 3 and 4 improved

emergence in all species except wild oat. Hand weeding ensured only species of interest existed within each plot and periodic irrigation promoted healthy crop/weed growth.

Table 3.3 Crop (canola, pea and wheat) and weed (redroot pigweed and wild oat) treatments designated for laboratory and field plot experiments.

#	**Treatment**	**Abbreviation ***
1	canola monoculture	CAN
2	pea monoculture	PEA
3	wheat monoculture	WHT
4	redroot pigweed monoculture	RRP
5	wild oat monoculture	WO
6	canola / redroot pigweed mixture	CAN / RRP
7	canola / wild oat mixture	CAN / WO
8	pea / redroot pigweed mixture	PEA / RRP
9	pea / wild oat mixture	PEA / WO
10	wheat / redroot pigweed mixture	WHT / RRP
11	wheat / wild oat mixture	WHT / WO

*Abbreviated names are used in further reference to crop and weed treatments.

Table 3.4 Planting dates for crop/weed plots in 2005 field season.

Trial	**Seeding Date**	**Notes**
1	May 5	RRP emerged late.
2	May 31	Flooding killed PEA and RRP did not emerge.
3	July 6	Excellent emergence in most species due to hand watering.
4	July 19	Excellent emergence of all species.

3.5 Image Acquisition Protocol

3.5.1 Lab Data Acquisition

The hyperspectral camera system was used to acquire image data (400-1000 nm at 10 nm intervals) of each greenhouse-reared treatment. Placement of the sensor, nadir to the plant samples, at a distance of 1 m resulted in a spatial resolution of 1.25 x 1.25 mm.

Samples were artificially illuminated using a single 500 watt halogen lamp placed at a constant distance from the plant samples. The light source was set at an angle of 27° off nadir, similar to the Solar Zenith Angle (SZA) of a mid-July day at 1:00 pm. Collection of hyperspectral data from sample trays assisted in camera system troubleshooting, development of acquisition protocols and provided imagery for evaluation of hue band thresholding and watershed segmentation.

3.5.2 Field Data Acquisition

The same hyperspectral camera system used in the lab experiment was placed on a boom arm, mounted on a flat-bed truck (Figure 3.5) and centered over each field plot at 1 m target distance. Imagery acquired from each plot was of 1.25 mm x 1.25 mm spatial resolution over the 400 – 1000 nm spectral range at 10 nm intervals. Image data were acquired at nadir ± 2 hours from solar noon (approx. 11 am-3 pm) under clear sky conditions to reduce the illumination intensity variation associated with changes in SZA and intermittent cloud cover. Data acquisition was limited to days of negligible wind to minimise leaf movement during plot imaging.

Figure 3.5 Flatbed Truck with sensor system boom.

Treatments seeded on July 6, 2005 provided temporal sampling as image data were acquired at approximately 1, 2, 3 and 4 weeks (July 14, 19, 26 and Aug. 3, respectively) after seeding. The July 19 and 26 acquisition dates encompassed the timeframe of optimal plant growth stage for herbicide application and thus were the focus in this study. The field-based plot image data provided data representative of real field conditions and were used for further investigation of threshold techniques (using Vegetation Indices (VI)) and evaluation of ANNs and MLC.

3.6 Image Segmentation

Two image segmentation techniques were investigated in this study. The first method, a simple threshold of a single band for identification of foreground (vegetation) pixels and creation of a vegetation mask, aids in simplifying the classification problem

through elimination of background pixels. The second method, watershed segmentation, was evaluated for efficiency in defining individual leaves within the image data, from which leaf shape variables could be extracted. As leaves of many weed and crop species differ in shape, potential exists for species discrimination based on shape characteristics. The following subsections explain these segmentation procedures in detail.

3.6.1 Thresholding

Hue Threshold

The hue colour component, which represents the dominant wavelength (relating to colour) (Lillesand and Kiefer, 1987) and human perception of colour (Cheng et al., 2001) was calculated from laboratory image data from RGB colour space. An IDL function, adapted from the method described by Foley and Van Dam (1982), was used to obtain hue values from red (670 nm), green (550 nm) and blue (450 nm) image wavebands. The range of hue values output from this function ranged from 0-360° with green centered at 120°, blue centered at 240° and red at 0° or 360°. Extracting the mean and standard deviation for green plant matter from the hue band, a threshold range of 90–160° was identified as vegetation and assigned a value of 1, all other values were assigned 0 and considered background.

The resultant threshold image contained a number of erroneous pixels that were removed with a series of erode then dilate morphological operators (Haralick et al., 1987) using a 3 x 3 circular filter kernel (Figure 3.6). The erode function removes pixels that fit inside the structural element (kernel) as it is passed over the image, thereby removing the noise pixels and consequently reducing the size of the areas of interest. Through applying the dilate function, existing features in the mask are returned to their original size. These

operators used in sequence eliminate isolated pixels while maintaining feature boundaries.

0	1	0
1	1	1
0	1	0

Figure 3.6 Circular structural element used in morphological erode and dilate procedures on vegetation mask for noise removal.

MCARI Threshold

A second method was developed for defining vegetation pixels based on image data acquired over field-based crop and weed treatments. Several Vegetation Indices (VI's) were evaluated for separating vegetation and background. The best separation was observed in the Modified Chlorophyll Absorptance Reflectance Index (MCARI) (Equation 3.3) image (Daughtry et al., 2000). The MCARI threshold method assigned pixel values ranging from 0.1 to 2.0 as green plant matter and values below 0.1 were non-vegetated and therefore not of interest. MCARI is calculated as:

$$MCARI=[(R_{700}-R_{670})-0.2*(R_{700}-R_{550})]*(R_{700}/R_{670}) \quad (3.3)$$

where R_{550} is reflectance at 550 nm, R_{670} is reflectance at 670 nm and R_{700} is reflectance at 700 nm.

3.6.2 Watershed Segmentation

The watershed segmentation algorithm was run (using IDL) to segment individual leaves from laboratory acquired image data. Prior to segmentation, the hue band was quantized to reduce the data range in the imagery. Reduction of data range has a smoothing effect, reducing small variations in the image surface. Because over-

segmentation is stated as an issue with this algorithm (Li et al., 1999; Ruberto et al., 2002), the reduced surface variability improved results.

Vegetation in the hue image is lighter than the background and inversion ensures the watershed algorithm interprets vegetation as basins on the image surface. The segmentation was applied on the original 8-bit (256 shades), quantized 4-bit (16 shades) and 3-bit (8 shades) image representations. The final step involved application of a vegetation mask (see hue threshold above) to the watershed output, masking background pixels and highlighting areas of interest in the imagery.

3.7 Manually Defined Leaves

Experimental analyses required that individual leaves be manually digitized to provide a dataset of known species class to be used in classification training and validation. These Regions Of Interest (ROIs) were defined from image data collected on both July 19 and 26 (Table 3.5). The plant stages on July 26 resulted in greater crop and weed ground cover, and allowed a larger number of pixels to be defined for all plant species except WHT. The total number of ROIs and associated pixels for each species are given in Table 3.6. This large database of image pixels were sub-sampled for statistical analyses (Analysis of Variance (ANOVA), PCA, SDA) and providing training and validation sets for the supervised classification techniques MLC and ANNs.

Table 3.5 Manually defined ROIs for both image acquisition dates.

	July 19		**July 26**	
Crop/Weed	**# Crop ROIs**	**# Weed ROIs**	**# Crop ROIs**	**# Weed ROIs**
CAN / RRP	29	55	30	43
WHT / WO	35	16	25	10
PEA / WO	22	20	21	33
WHT / RRP	42	60	55	36
CAN / WO	45	19	24	15
PEA / RRP	20	57	20	35

Table 3.6 Total number of ROIs and their associated pixels for each weed and crop species investigated.

	July 19		July 26	
Species	**# ROIs**	**# Pixels**	**# ROIs**	**# Pixels**
CAN	64	23,899	53	62,082
PEA	42	11,007	41	15,437
WHT	77	6,932	80	6,416
RRP	171	12,161	114	22,438
WO	45	2,299	58	3,434

3.7.1 Classification Training

The two supervised classification methods (MLC and ANN) required input data of each species for training. Particular attention was given not only to representation of species spectrally, but also spatially across each image scene. Each image was divided into nine equal sections. Training samples (ROI leaves) were selected (1-4 regions per section, based on leaf size) from each section equally across the plots (for example, CAN leaves were sampled from both the CAN/WO and the CAN/RRP treatments). This ensured that any sensor variation across the image scene would be represented in the classification training dataset. With selection of leaf regions complete, a one of n sampling procedure reduced the training set to approximately 500 pixels for each species (Table 3.7).

Table 3.7 Number of ROI training samples and associated pixels selected for classification training. Subset pixels selected by 1 of n sampling.

Species	# ROIs	ROIs/Section	Total # pixels	Subset Pixels
July 19 Acquisition				
CAN	9	1	5334	649
RRP	36	4	3287	532
PEA	18	2	4424	562
WHT	36	4	3454	591
WO	36	4	1906	488
July 26 Acquisition				
CAN	9	1	9701	648
RRP	36	4	7577	542
PEA	18	2	6891	573
WHT	36	4	3545	590
WO	36	4	2434	488

Training pixels used for classification of the July 19 and 26 image data were also combined into a multitemporal training set in order to encompass/represent the temporal variability, observed between these two dates. This resulted in approximately 2000 pixels (1000 weed and 1000 crop) used as input to train the multitemporal series classifications.

3.7.2 Classification Validation

Classification accuracy assessment requires samples independent from the training set. Elimination of leaves used for training from the manually defined leaves created an independent validation set (Table 3.8). As classifications were run on a per plot basis, the validation sites could not be defined across treatments as was the case in training. Class validations were tabulated as contingency tables using the post classification modules in ENVI/IDL. Results are presented as overall classification accuracy, Kappa coefficient and errors of omission and commission, which were computed from contingency tables (Jensen, 1996).

The error of omission represents the probability of a reference pixel being correctly classified while commission error is the probability that a classified pixel actually belongs to that class. Overall accuracy represents the percentage of pixels classified correctly in the entire validation set while the Kappa coefficient takes into account not only overall accuracy but also the omission and commission errors. These standardized methods of accuracy assessment provide comparison between the two supervised methods as well as between single date, multitemporal and reduced waveband classification series.

Table 3.8 Pixels used for validation of field plot classification output.

Crop / Weed	# Crop Pixels	# Weed Pixels
July 19		
CAN/RRP	10268	2839
WHT/WO	1869	62
PEA/WO	2804	268
WHT/RRP	1301	2739
CAN/WO	8222	27
PEA/RRP	3763	3384
July 26		
CAN/RRP	35008	5101
WHT/WO	975	339
PEA/WO	4101	358
WHT/RRP	1887	4684
CAN/WO	17379	292
PEA/RRP	4451	5076

3.8 Image Statistics

Selection of pixels for statistical analyses involved application of a random number to the data records, sorting based on these random numbers and selection of the first 1000 pixels for each species. Twenty repetitions of ANOVA and SDA procedures were run using SAS statistical software (SAS Institute Inc., Cary, NC, USA), each with a

new set of randomly selected pixels. These repetitions ensured that error caused by sample selection would be reduced, and therefore increase confidence in analysis results.

3.8.1 Analysis of Variance

The ANOVA procedure was used to identify significant differences amongst species reflectance in each waveband. Significant difference was measured at the 95% confidence level with the p-value output from the SAS procedure. A p-value of less than 0.05 suggested that a significant difference existed amongst mean species reflectance at each waveband. Plots (x = band, y = p-value) enabled visualization of the discriminatory bands and more importantly identified bands which had little discriminatory power.

3.8.2 Stepwise Discriminant Analysis

In addition to ANOVA, SDA was run to identify bands of particular discriminatory power. The SDA first began without variables in the discriminatory set. Through an iterative process, variables were either entered or removed from the set based on the reduction of the Wilk's lambda statistic at a specific confidence level (0.05). The process ran, continually adding or removing wavebands until no further entry or removal of variables caused a further reduction of Wilk's lambda. The final output was a list of wavebands ranked by discriminatory power amongst species.

Typically, the number of wavebands selected ranged from 20-30 (of the original 61) depending on the classes tested in the model. For selection of the most important wavebands, the Wilk's lambda output was plotted (x = iteration, y= Wilk's lambda value) and the iteration at which the plot began to plateau (delta Wilk's lambda < 0.01 and <0.005) was identified (Figure 3.7). The bands defined at these iterations were recorded

and counted over the twenty repetitions of the SDA to produce plots (x=band, y=count) of consistently selected discriminatory bands.

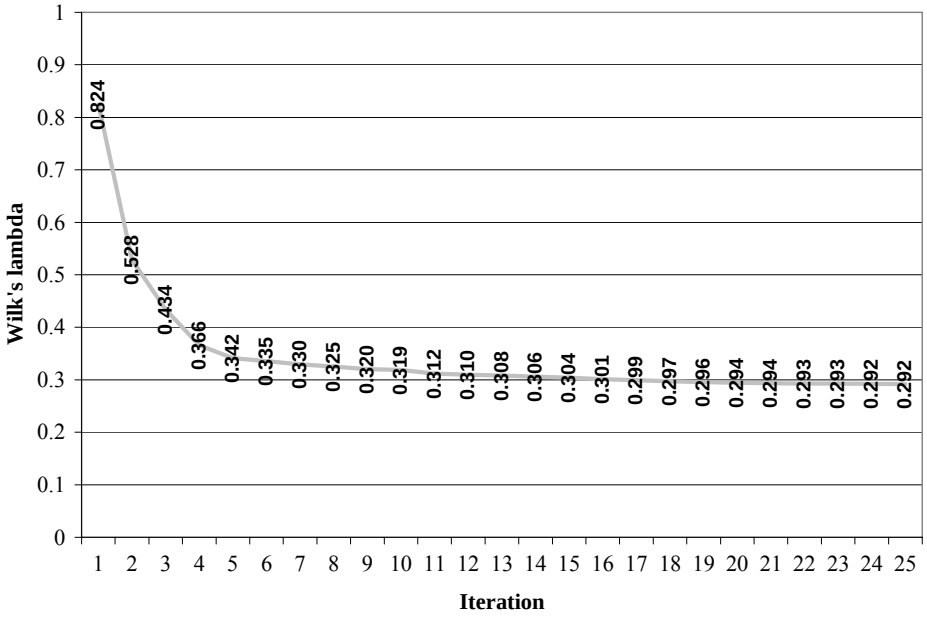

Figure 3.7 Reduction of Wilk's lambda statistic for a single stepwise discriminant run of CAN vs. RRP. The line begins to plateau at iteration 6 (delta <0.01) and iteration 9 (delta <0.005).

3.8.3 Principal Components Analysis

PCA is a mathematical transformation in the spectral domain, and is typically used to produce uncorrelated output bands, segregate signal noise and reduce dimensionality of remotely sensed image data (Jensen, 1996). The components are linear combinations of the original wavebands, created by transformation coefficients derived from the covariance matrix of the original image data. These coefficients include eigenvalues which represent the half-lengths of the principal axes and eigenvectors which represent the orientation of the principal axis. Eigenvalues of the transformation represent the amount of total variance contained within the component. The component

with the highest eigenvalues therefore account for the most variance in spectral space and are considered to contain the most information.

Each component receives some contribution from all of the original image wavebands. This contribution can be calculated through examination of the eigenvectors, as the magnitude of each element in the vector is directly proportional to the input wavebands' contribution. By calculating the percent contribution of the original bands to each component with the highest eigenvalues, bands from the original image data can be defined as containing the non-redundant information with respect to spectral discrimination.

PCA was run using the ENVI/IDL software package. Prior to the analysis, the image data were masked to include only the crop/weed combinations of interest. The percent contribution of each input band to the first three components were calculated (Equation 3.4) and plotted (x = band, y = % contribution). The bands identified as contributing most to these components further aided selection of important bands for discriminating crop and weed species. The % contribution was calculated as:

$$\%Contribution = (i_b^2 / \sum_{i=1}^{61} i^2) * 100 \qquad (3.4)$$

where i is the eigenvector element and b is the input band.

3.9 Image Classification

Image classification procedures aim to generalize image data by defining classes and assigning each pixel to a class based on spectral characteristics. In this study, two classification techniques (MLC and ANN) were evaluated for the potential to discriminate between single crop/weed species combinations. The application of the

MCARI vegetation mask identified only vegetation pixels which further simplified the classification problem. Because these two techniques are supervised, training data (*see* Section 3.6.1) were defined from the manually defined ROIs and subset with particular attention to representation of species spectral and spatial variability.

3.9.1 Maximum Likelihood Classification

Three series of MLC were conducted using ENVI/IDL software. The ENVI MLC procedure does a calculation of the class covariance matrices of each species from training pixels. Training statistics were computed for classification of single dates (July 19 or 26) as well as multitemporally, in which training pixels were combined across the two acquisition dates and these covariance matrices were used in classification of weed/crop field plot image data from July 19 and 26. A reduced number of bands, identified from the ANOVA, PCA and SDA were used as input to the MLC. This set was run on the July 19 image data and was used to evaluate the effects of a reduction in spectral dimensionality on classification output.

3.9.2 Artificial Neural Networks

ANN models were developed using the same classification series as above (single date, multitemporal, and reduced bands). Feed-forward ANN modelling was conducted using Predict® v3.11 (NeuralWare Inc., Pittsburgh, PA) software. This involved: 1) selecting internal validation, training and internal test data subsets, 2) analyzing and transforming data, 3) selecting variables, 4) network construction and training, and 5) model verification. The ANN software partitioned the data from the training set into subsets as follows: 30% of these data were removed to form an internal validation set,

with the remaining 70% were further partitioned 70% / 30% into training and internal test sets, respectively. The training set was used to develop ANN models and the internal test set to adjust ANN parameters during training. The 30% internal validation set was held separate during training, and then used as an initial evaluation of ANN model performance.

Five networks were developed using the above procedure with the best model selected, based solely on internal validation performance. This was then run over 20 iterations which produced 20 (best of five) network models for each crop/weed combination. These 20 networks were evaluated based on the following factors:

Network Architecture – The ANN models consist of three layers, the input, hidden and output (2 classes). Each of the 20 models was evaluated such that the hidden layer contained approximately half of the number of nodes as the input layer. Once these models were defined, the validation (internal and external) performance was investigated.

Validation Performance – Models with highest internal and external validation accuracies were identified. The internal validation accuracy was set at a lower priority than the external validation because the independent external samples suggest a better representation of real world accuracy assessment.

Once the best model of 20 was identified for each crop/weed combination, the field plot treatments were classified. Each pixel within the plot image was fed into the network model with the output class used to reconstitute these data into a classified image. The classed image was then validated based on manually defined regions independent of training.

CHAPTER 4 RESULTS

4.1 Introduction

Initial investigation into segmentation methods was conducted on laboratory image data of greenhouse grown crop and weed plants. Two objectives, segmentation of individual leaves through watershed transformation and segmentation of vegetation pixels from image background through hue thresholds, were investigated. Upon acquisition of field-based weed and crop treatments, an extension on this technique using vegetation indices was investigated. These segmentation methods identified vegetated pixels that could then be analyzed statistically and passed to the classification algorithms.

Descriptive statistics (mean and standard deviation) and ANOVA were run on image data acquired over field-based crop and weed treatments to characterize important areas of the EM spectrum for species discrimination. The SDA and PCA were used to select a subset of wavebands to form a multispectral dataset for the reduced band classification series run on the July 19 image data.

Two supervised classification techniques (ANN and MLC) were evaluated for species identification accuracy through three series of classifications: single date, multitemporal and single date with a reduced number of wavebands. The first series involved single date classifications using the entire 61 waveband image dataset and tested the accuracy of classification from a single image acquisition. With two dates (July 19 and 26) available, a second series of classifications were trained using data from both acquisitions. This multitemporal series provided an evaluation of classification accuracy, accounting for not only spatial, but also temporal variation in leaf reflectance

characteristics. The third series of classifications investigated the need for a full hyperspectral dataset versus a subset of narrow wavebands representative of image data provided by a multispectral system. Using a reduced subset of wavebands identified through statistical analyses, an evaluation of classification accuracy for July 19 image data was conducted. Additional perspectives on results and implications to precision agriculture and SSHM are presented in Chapter 5.

4.2 Segmentation of Laboratory Image Data

Image data acquired in a laboratory setting using greenhouse grown plants provided a means to evaluate two image segmentation methods; thresholding of the transformed hue colour component and watershed segmentation. These image data included a wheat (WHT) plant, two canola (CAN) plants and several redroot pigweed (RRP) plants at various phenological stages (Figure 4.1). The different leaf shape and size represented in these images provided an initial evaluation for the segmentation procedures.

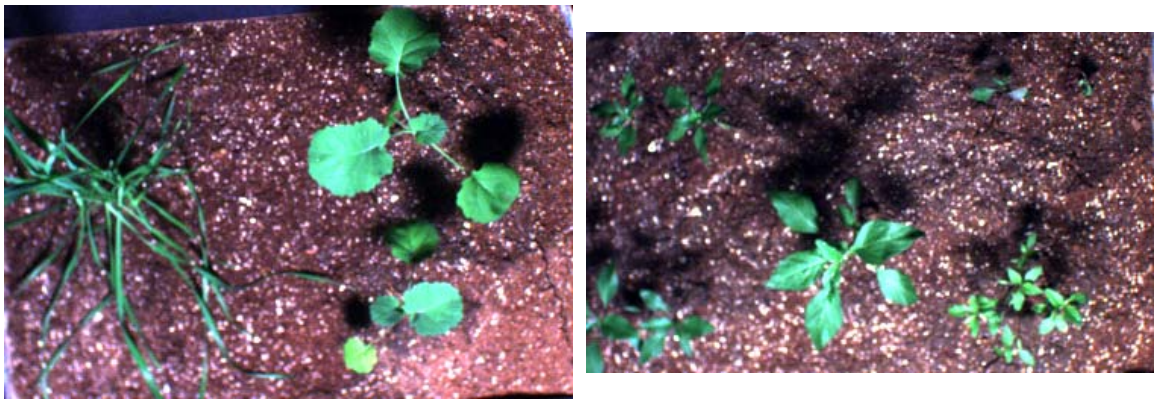

Figure 4.1 Laboratory acquired WHT and CAN (left) and RRP (right) image data used for testing segmentation procedures.

4.2.1 Hue Threshold

The two laboratory images were converted to the hue colour component (Figure 4.2a). All pixels with hue values between 90-160° were assigned a value of 1 and the remaining pixels assigned a value of 0 (Figure 4.2b). This threshold of the hue component produced some spurious pixels in areas where vegetation did not exist. Using morphological erode and dilate filters removed spurious pixels then expanded leaf boundaries back to their original size (Figure 4.2c) (Haralick et al., 1987).

The hue threshold procedure was accurate in identifying green plant matter in both crop and weed images. Regardless of reflectance variability due to leaf angle, it was possible to identify foreground vegetation pixels. WHT and RRP showed a high degree of leaf overlap, which confounded identification of single leaf segments. The CAN plants, characterized by widely spread leaves, were segmented relatively well, though connecting petioles resulted in a single region being defined for the entire plant rather than a single leaf region.

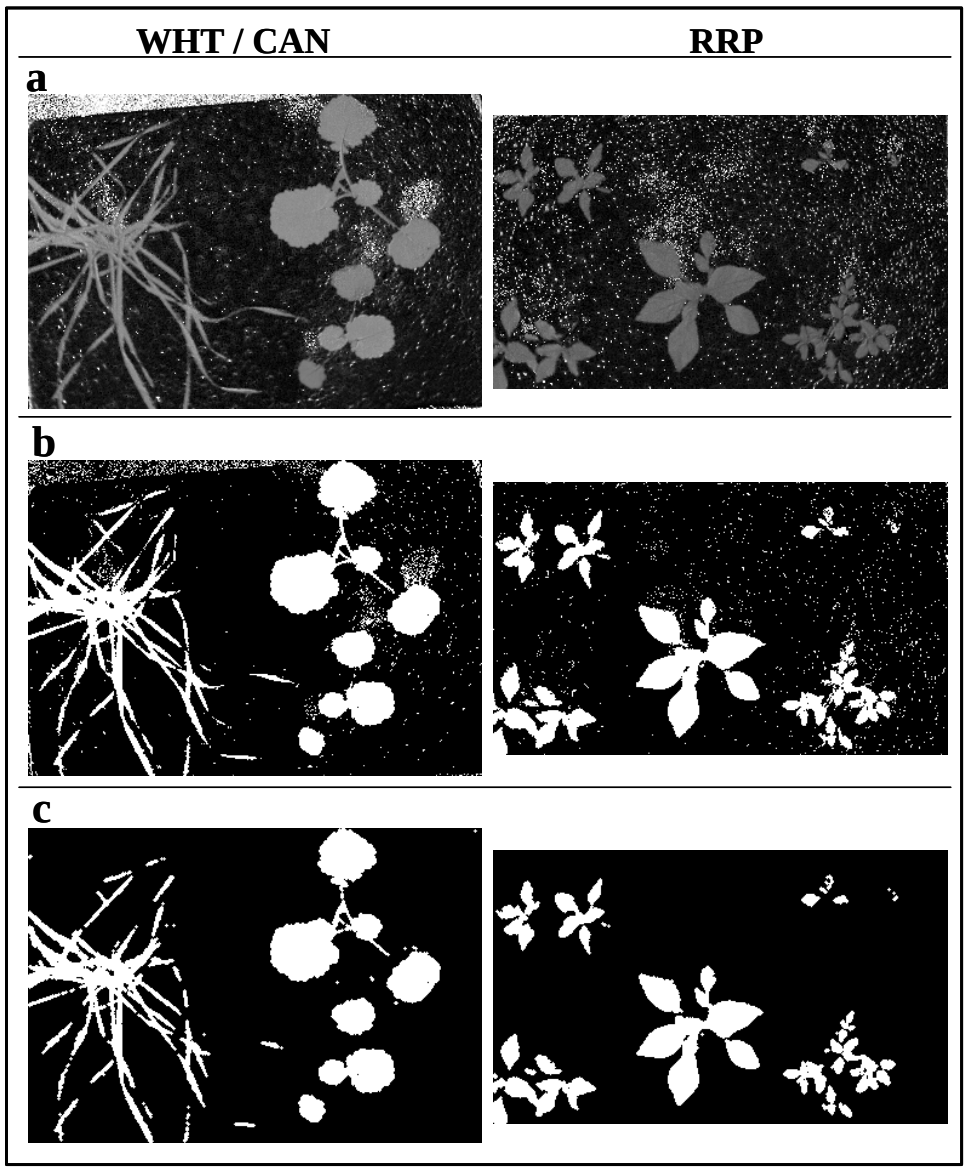

Figure 4.2 Processing steps in creation of vegetation mask for both WHT/CAN and RRP treatments: (a) hue colour component; (b) 90-160° threshold image; (c) the result of the erode and dilate operators.

4.2.2 Watershed Segmentation

The watershed segmentation algorithm was evaluated for potential in defining individual leaf segments from transformed hue image data acquired in the laboratory. This was a preliminary step to measuring leaf shape characteristics. Over-segmentation

(excessive small segments within each leaf) for WHT, CAN and RRP was evident in the watershed output using the original 8-bit (256 grey-levels) images (Figure 4.3a). Output from the 4-bit hue imagery (Figure 4.3b), resulted in the definition of larger regions for all three species such that fewer regions defined a single leaf. Reducing the data range to 3-bit (Figure 4.3c) further improved the segmentation results, as defined leaf regions were larger and less affected by local hue variation across the leaf surface, though defined segments extended past leaf boundaries. Since the vegetation mask created by hue thresholding was accurate in detecting plant edges, optimal results were obtained in terms of individual leaf segmentation by applying the hue threshold mask to the watershed transformation output.

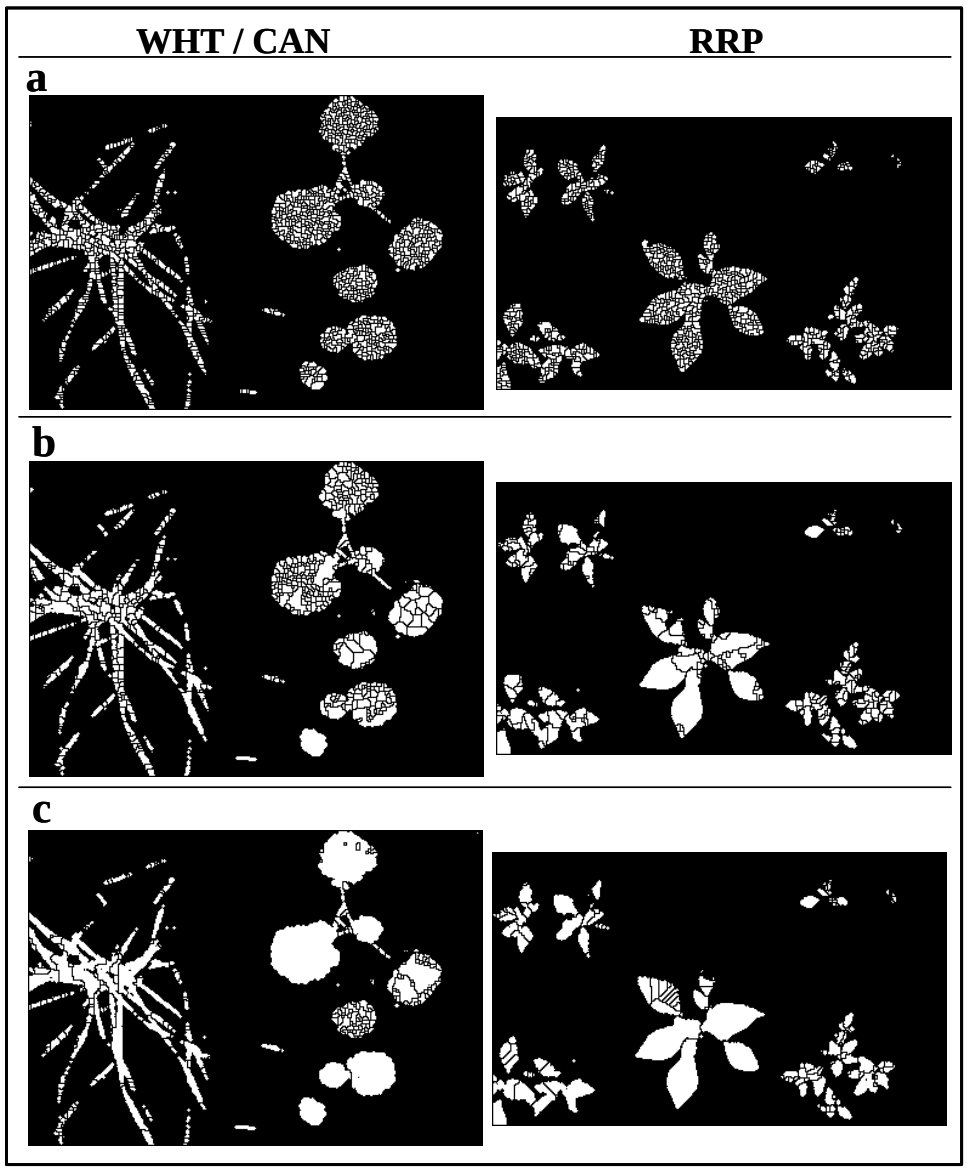

Figure 4.3 Watershed segmentation results of WHT/CAN and RRP treatments on: (a) 8-bit; (b) 4-bit; (c) 3-bit hue bands.

This initial evaluation of the watershed segmentation showed that it was not well suited to defining individual leaf segments. Leaf overlap and over-segmentation made shape measurement impossible with this dataset, therefore this method was not investigated with field plot image data.

4.3 Segmentation of Field Image Data

Since encouraging results were obtained in defining vegetation pixels using thresholds, this method was further investigated on the field image data. The availability of NIR wavebands in these data enabled evaluation of VI thresholding. Through visual examination of 13 VIs, the MCARI (Daughtry et al., 2000) index provided the best separation between foreground (vegetation) and background (soil, litter) pixel values, and was consistent across the multiple weed/crop combination plots on the two image acquisition dates (July 19 and 26).

4.3.1 MCARI Threshold

Defining the minimum MCARI value for vegetation was achieved through manual identification of vegetation pixels in the image data. The lowest observed MCARI value for sunlit and shadowed vegetation pixels in the images was 0.1. Leaf edge pixels affected by background mixing showed a MCARI value lower than 0.1 and was defined as the minimum value for the threshold. Assigning all pixels with values $\geq$ 0.1 as foreground (set to 1) and all others as background (set to 0), created the vegetation mask (Figure 4.4).

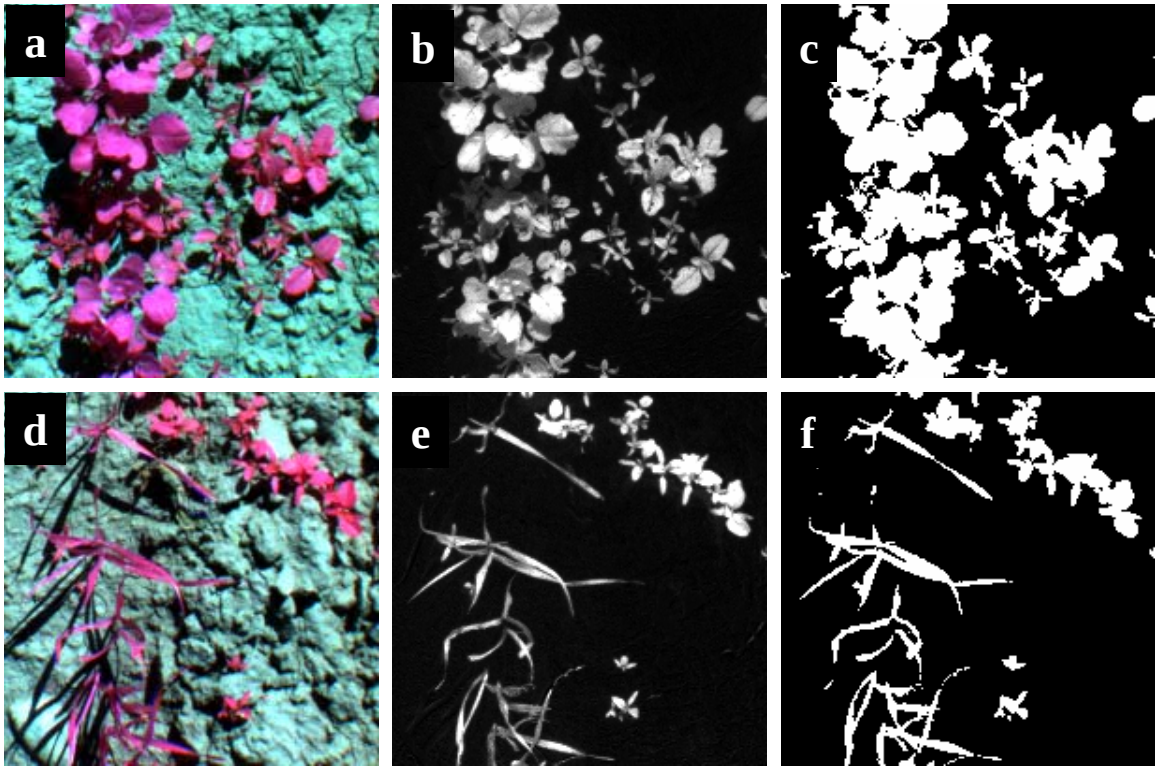

Figure 4.4 MCARI threshold technique for segmenting vegetation ((a) CAN/RRP and (d) WHT/RRP) from background. MCARI vegetation index is calculated (b,e) and a value of 1 was applied to all pixels with a value of > 0.1 to create a mask of only vegetation pixels (c, f).

MCARI thresholding efficiently defined vegetated pixels and this method was applied to all field-based image data acquisitions prior to classification as it eliminated the requirement of training for background classes. It is believed that processing efficiency was improved as only vegetation pixels were passed to the classification procedures. Prior to testing classification procedures, descriptive statistics (mean and standard deviation), ANOVA, SDA and PCA were run on image data acquired over field-based crop and weed treatments to characterize important areas of the EM spectrum for species discrimination.

4.4 Image Statistics

The mean reflectance of training pixels extracted from both the July 19 and 26 acquisition dates are shown in Figures 4.5 and 4.6, respectively. The greatest spectral difference was observed between the monocotyledon (WHT, WO) and dicotyledon (CAN, PEA, RRP) species, especially in the NIR region where reflectance differed by >10%. On the later date (July 26), WHT differed from WO in the visible portion of the EM spectrum, but mean reflectance in the NIR region was similar, suggesting that this monocotyledon combination may be difficult to classify based solely on spectral reflectance characteristics. CAN and PEA reflectance were also similar to RRP, though differences in the red-edge and NIR regions (700-1000 nm) were observed on July 19 between the respective crop and weed spectra and between PEA and RRP on July 26. The dotted lines in Figure 4.5 and 4.6 represent ±1 standard deviation from the reflectance mean and show the high variance in sampled populations. These variances about the mean of the training classes identified the complexity of separation between weed and crop species.

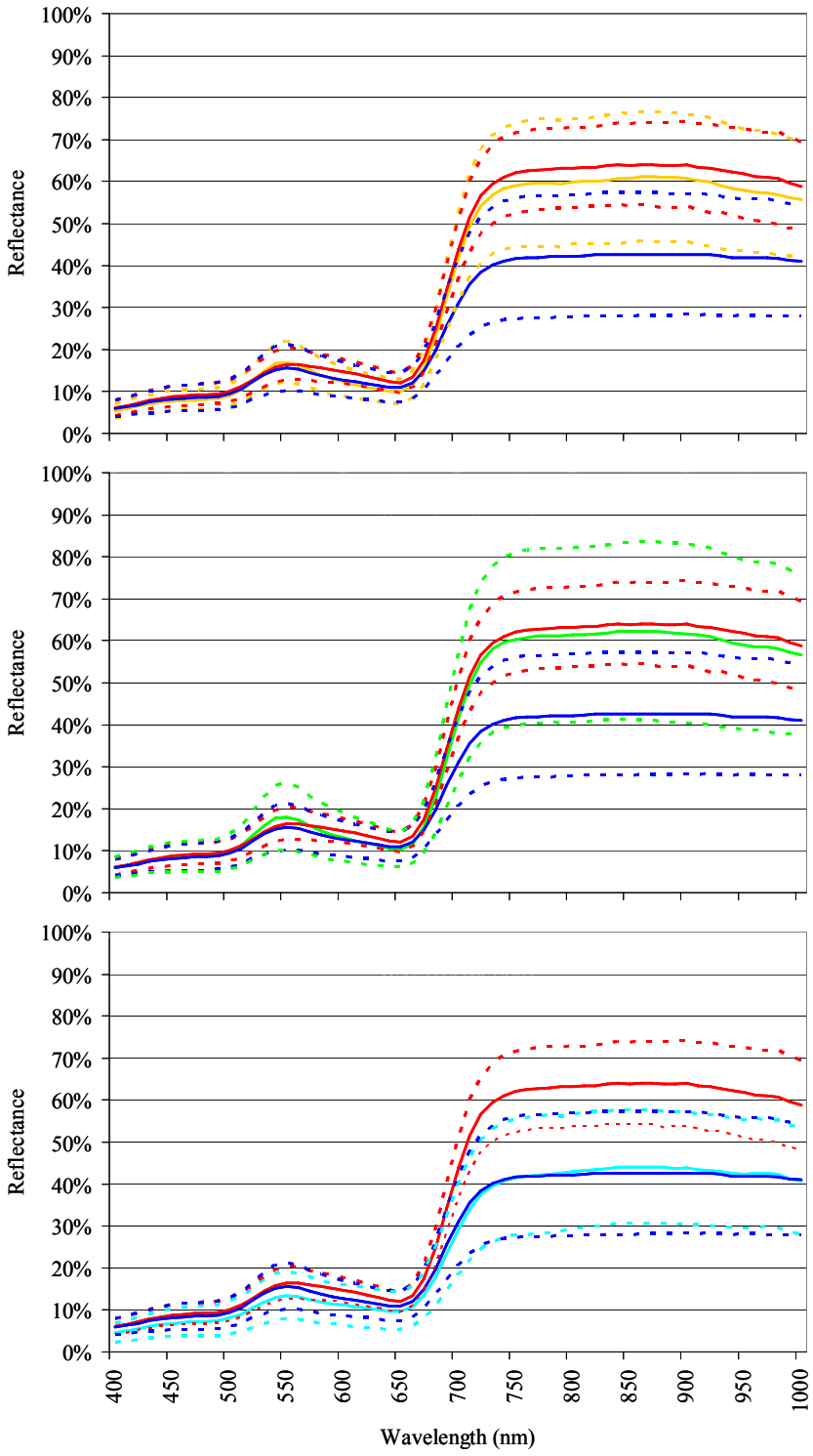

Figure 4.5 Mean reflectance of crop (CAN=orange, PEA=green, WHT=cyan) and weed (RRP=red, WO=blue) classes drawn from July 19 training data (Dotted Lines = ±1 Standard Deviation).

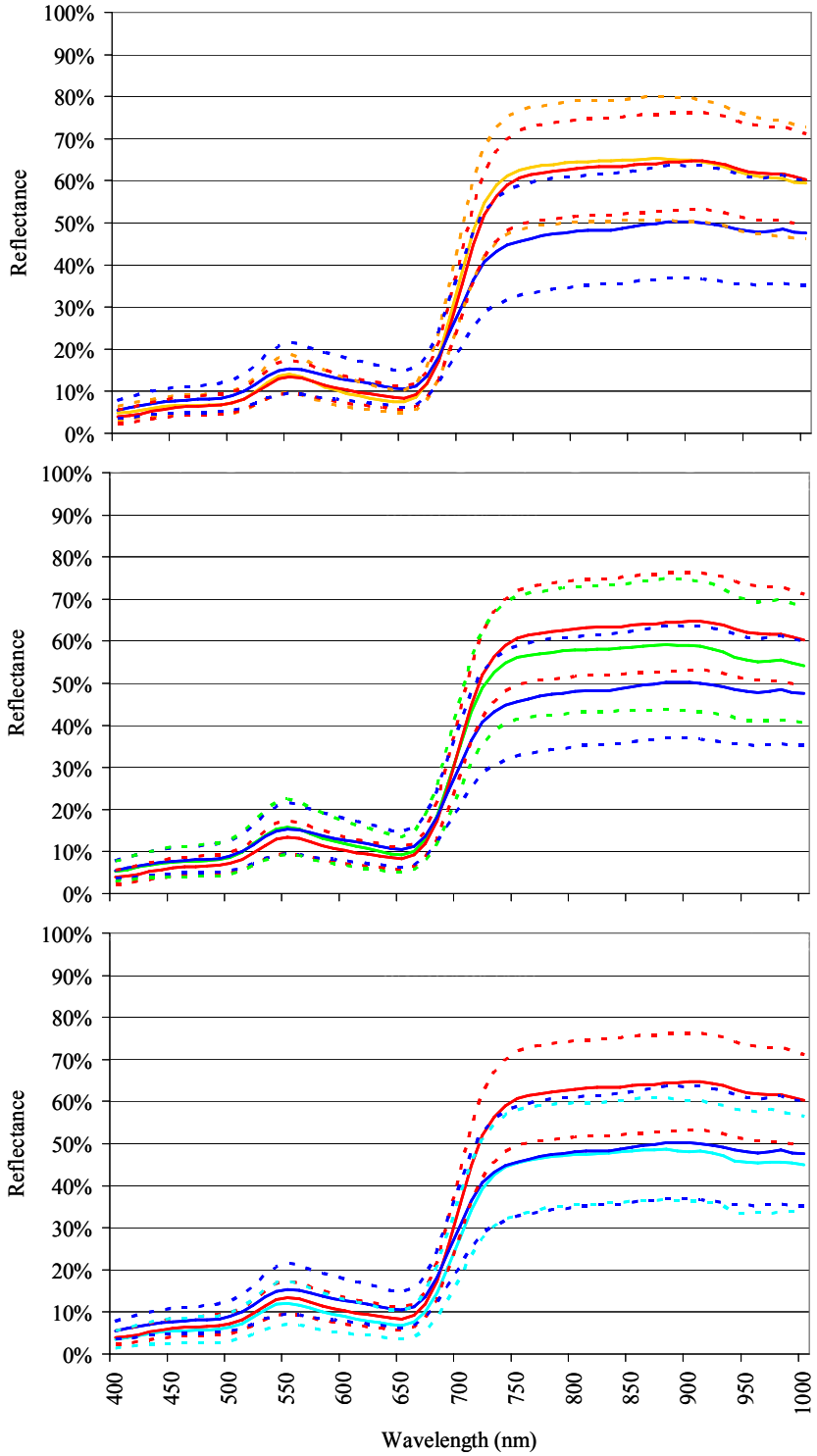

Figure 4.6 Mean reflectance of crop (CAN=orange, PEA=green, WHT=cyan) and weed (RRP=red, WO=blue) classes drawn from July 26 training data (Dotted Lines = ±1 Standard Deviation).

ANOVA statistics provided a method of testing for significant differences in the reflectance spectra between each crop/weed combination across all wavebands. Twenty repetitions (randomly selected subsets of 1000 pixels/species) of ANOVA were plotted for July 19 (Figure 4.7) and 26 (Figure 4.8). A probability value of <0.05 for a particular waveband indicated a significant difference (with 95% confidence) between the reflectance means of crop and weed species. For both acquisition dates, WHT and RRP reflectance means differed significantly over the entire measured wavelength domain (400-1000 nm). Significant differences were also observed for WHT and WO species on both dates except in the wavebands >800 nm on July 19, which was unexpected given the similarity in the species mean reflectance plots (Figure 4.5 and 4.6). The ANOVA results for PEA and CAN show that reflectance of the crop species were similar to the two weed species with the exception of those wavebands on either side of the green peak (510-530 nm and 570-590 nm). Sections of the NIR (700-800 nm and 850-900 nm) were not significantly different between the two broadleaf crops (PEA and CAN) and the RRP class, though differences were observed between WO and the two broad-leaf crops (with the exception of 690 nm).

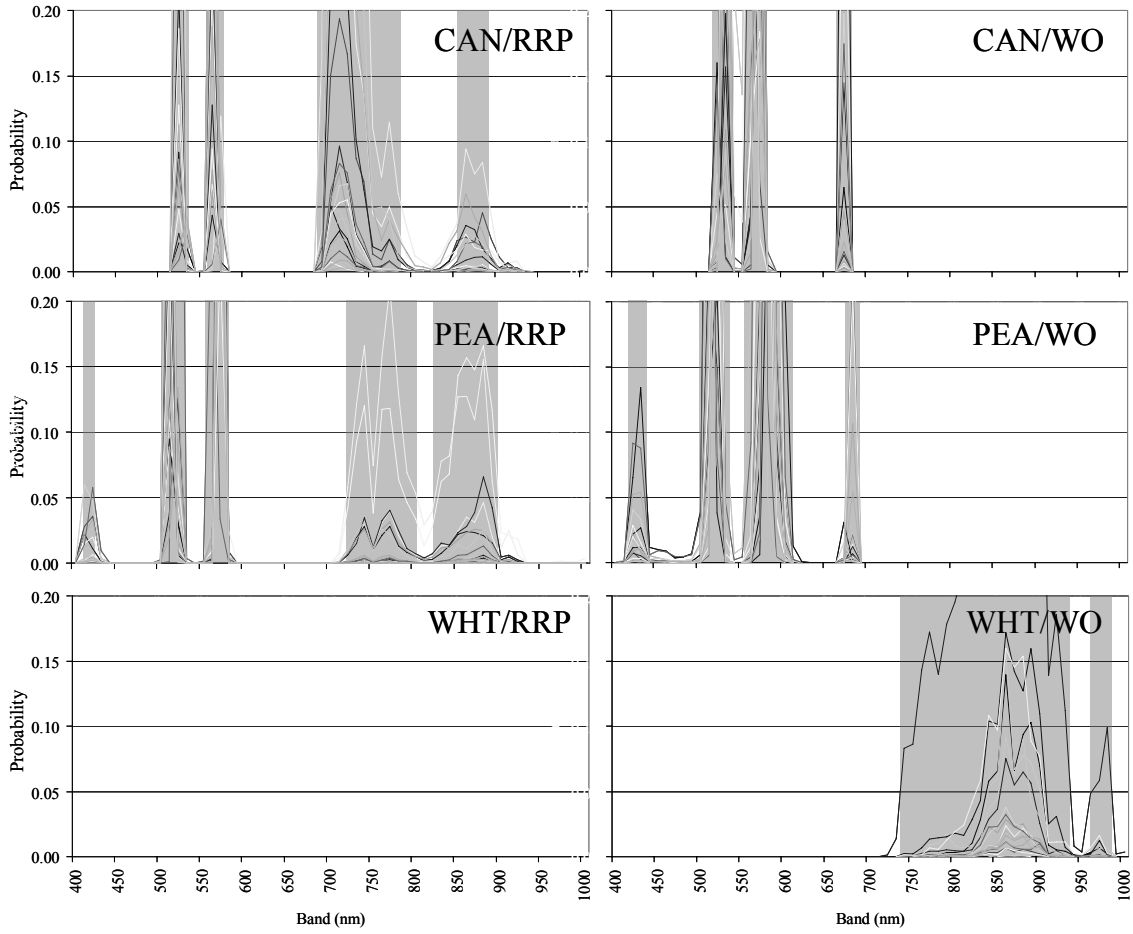

Figure 4.7 ANOVA probability values (over 20 repetitions) plotted by waveband for crop/weed combinations on July 19 acquisition date. Grey sections indicate wavelengths where no significant difference exists between weed/crop combinations.

On the later acquisition date (July 26) reflectance at 550 nm differed significantly between all weed crop combinations except CAN/WO. Similar to July 19, CAN and RRP reflectance did not show differences on either side of the green peak. In the case of CAN and WO and PEA and RRP, with few exceptions (550 nm and 700-730 nm respectively) reflectance differs significantly. In PEA and WO, reflectance differed significantly at 550 nm and also in the region 640-660 nm.

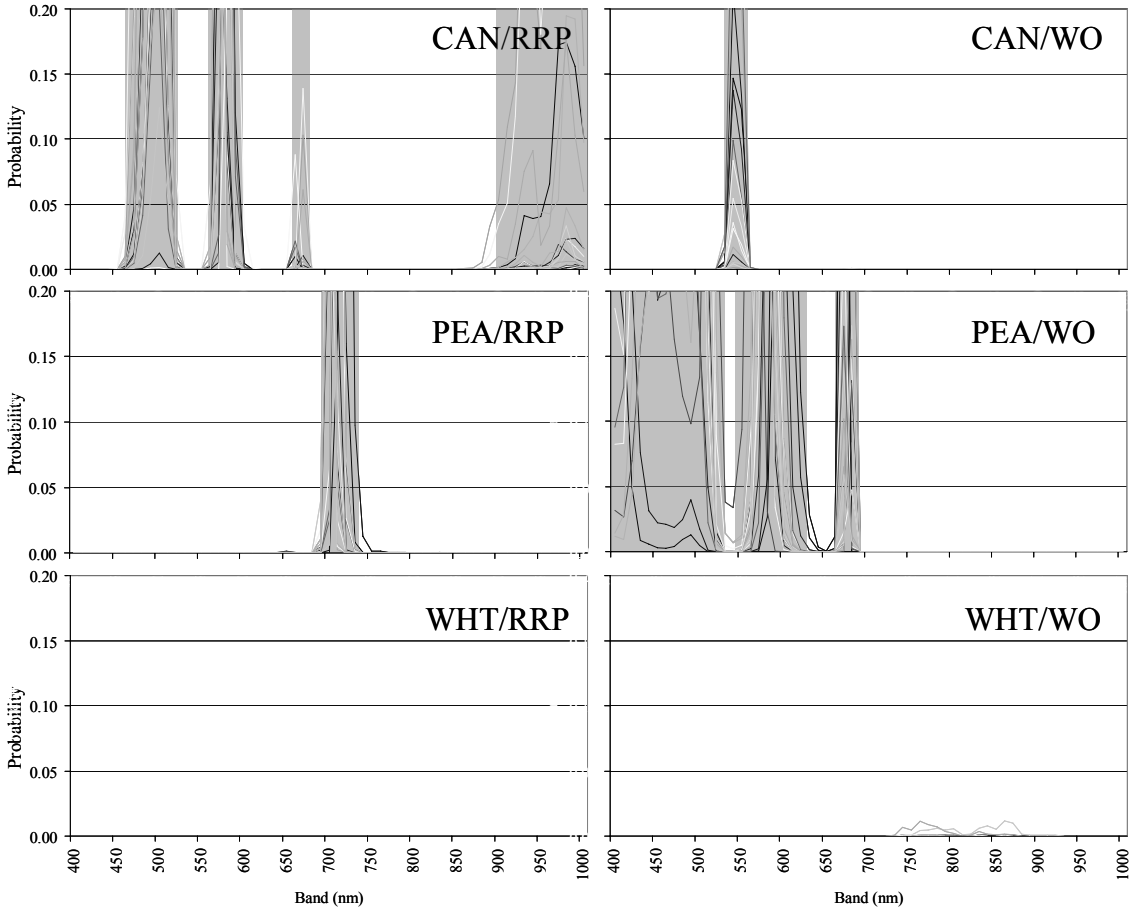

Figure 4.8 ANOVA probability values (over 20 repetitions) plotted by waveband for crop/weed combinations on July 26 acquisition date. Grey sections indicate wavelengths where no significant difference exists between weed/crop combinations.

4.5 Discriminatory Wavebands

SDA and PCA were used for identification of particular wavebands of importance in discrimination of crop and weed classes. Once selected, this subset of wavebands was used in the reduced band series of classifications run on the July 19 acquisitions.

4.5.1 Stepwise Discriminant Analysis

The SDA procedure identified the importance of each waveband for discrimination of crop and weed species. The selected wavebands of importance

constitute a subset of the original bands reducing the spectral dimensionality of image data needed for species discrimination. The SDA was run 20 times for each crop/weed combination using a different set of randomly selected pixels (1000 per class) each time. Output consisted of a ranked list of discriminatory wavebands, selected based on how their addition to the set reduced the Wilk's lambda statistic.

Two subsets of wavebands were selected from the ranked output list for each crop/weed combination. The first set included wavebands that reduced the Wilk's lambda by greater than 0.005, the second set reduced the Wilk's lambda by greater than 0.01. The number of times each waveband was selected (frequency of selection) over the 20 independent runs identified wavelengths that were consistently important in crop/weed discrimination for the July 19 acquisition (Figures 4.9 and 4.10).

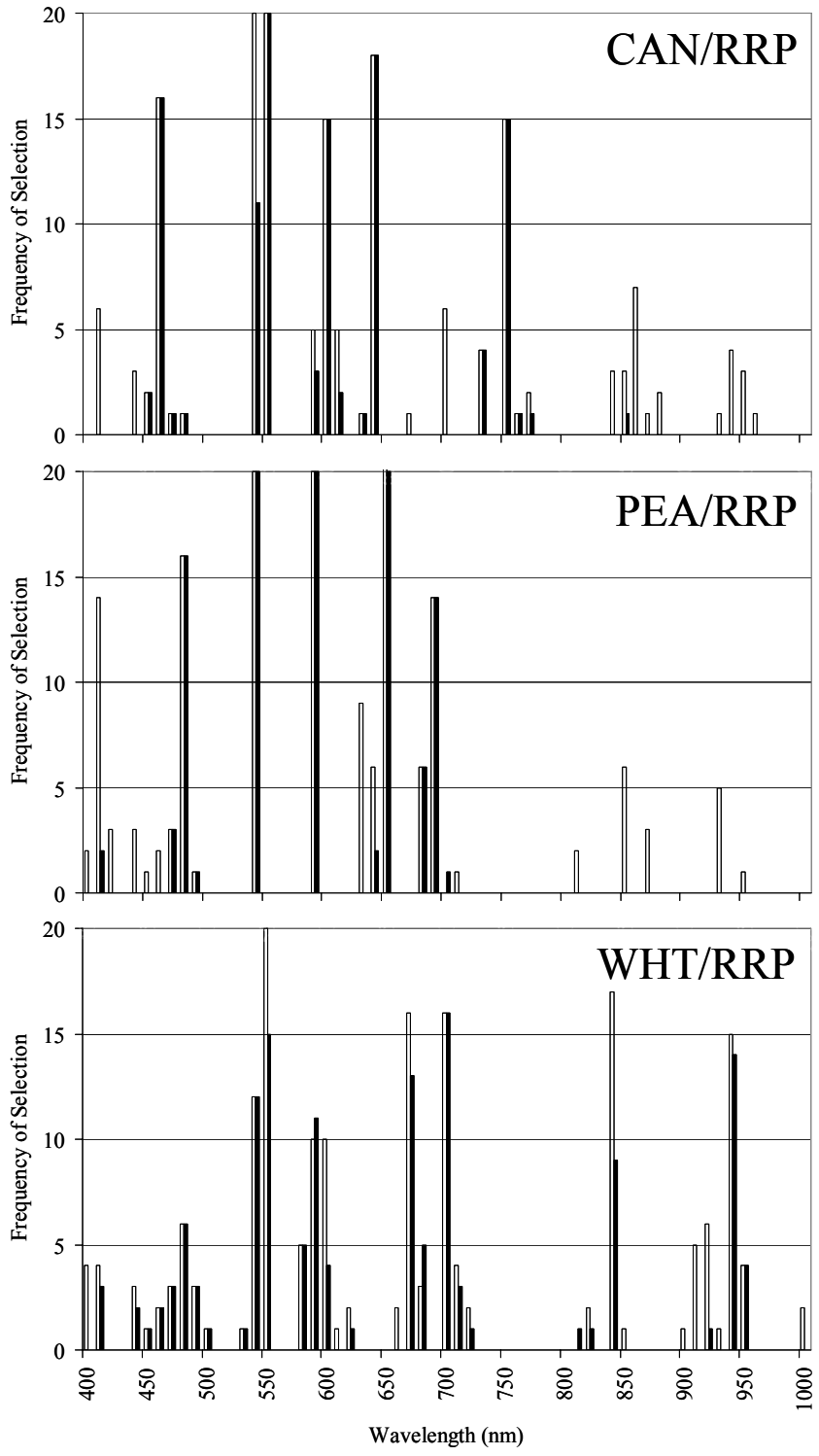

Figure 4.9 Count of selected discriminatory bands (over 20 repetitions) plotted by waveband for crop/RRP combinations on July 19 acquisition date. Black bars represent delta Wilk's lambda 0.01; white bars represent delta Wilk's lambda 0.005.

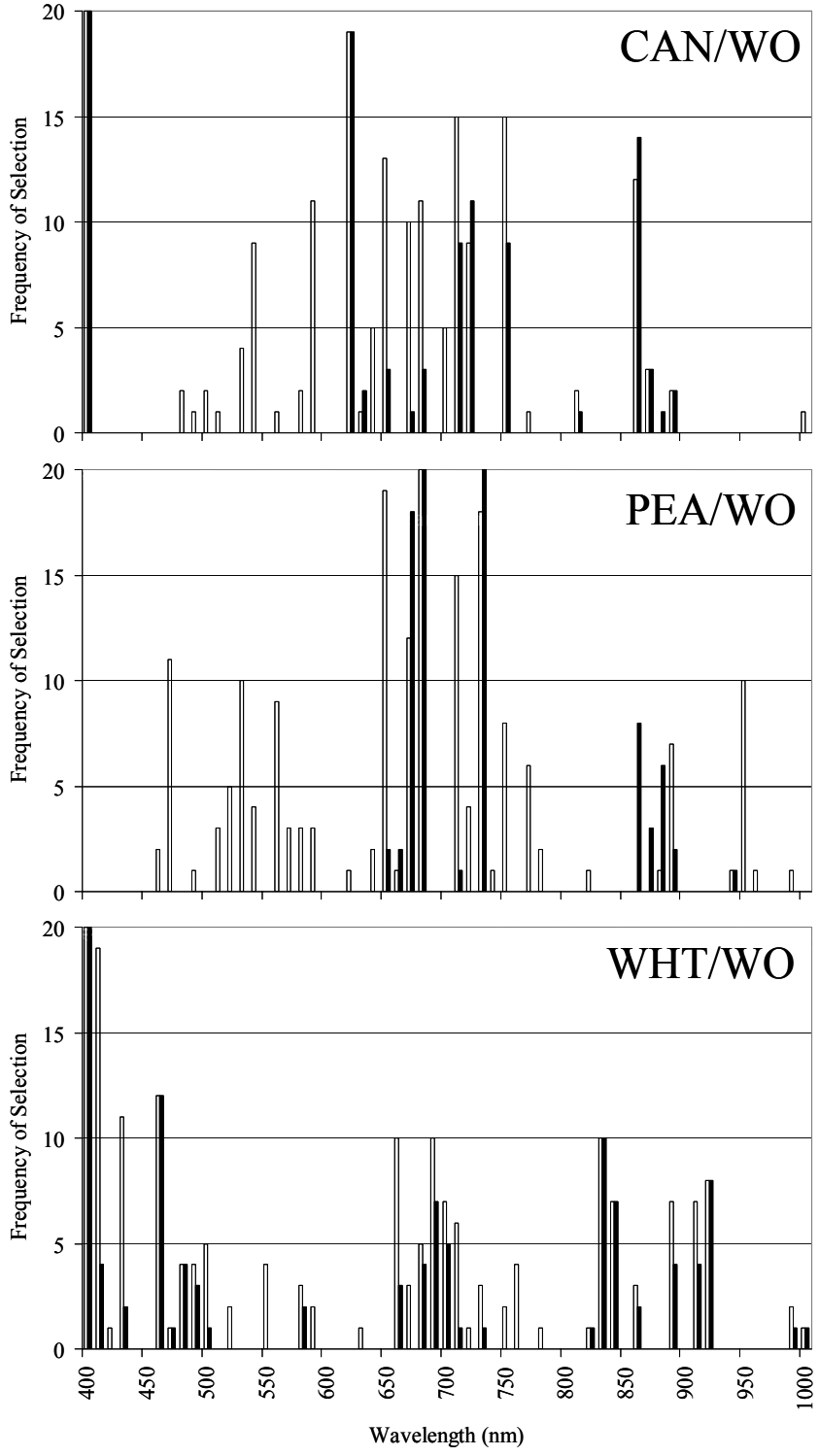

Figure 4.10 Count of selected discriminatory bands (over 20 repetitions) plotted by waveband for crop/WO combinations on July 19 acquisition date. Black bars represent delta Wilk's lambda 0.01; white bars represent delta Wilk's lambda 0.005.

The SDA of the dicotyledon crop/weed combinations (CAN/RRP and PEA/RRP) identified several wavebands situated in the visible spectrum (480, 550, 600, 640, 650, 660 and 670 nm) to be frequently selected, while those in the NIR portion of the spectrum were selected less frequently. The CAN/WO and PEA/WO combinations showed wavebands in the red, red-edge and NIR (620, 670, 720, 860 nm) regions to be of discriminatory importance while very few wavebands in the blue and green regions of the visible range were selected. The results for the monocotyledon WHT/WO combination showed wavebands in the range 400, 460-480, 670-700, 830 and 920 nm to be important in terms of discriminatory power. These same wavebands along with 840, 930, 940 and 950 nm were identified as important for the discrimination of WHT and RRP.

4.5.2 Principal Component Analysis

PCA was run 20 times for each crop/weed combination on image data acquired July 19. Calculation of the percent (%) contribution of each original waveband to the transformed component identified those wavebands containing the most information and therefore deemed most useful or important for species differentiation. Plotting the relative contribution of each original waveband to the first three components identified several regions of spectral importance (Figure 4.11).

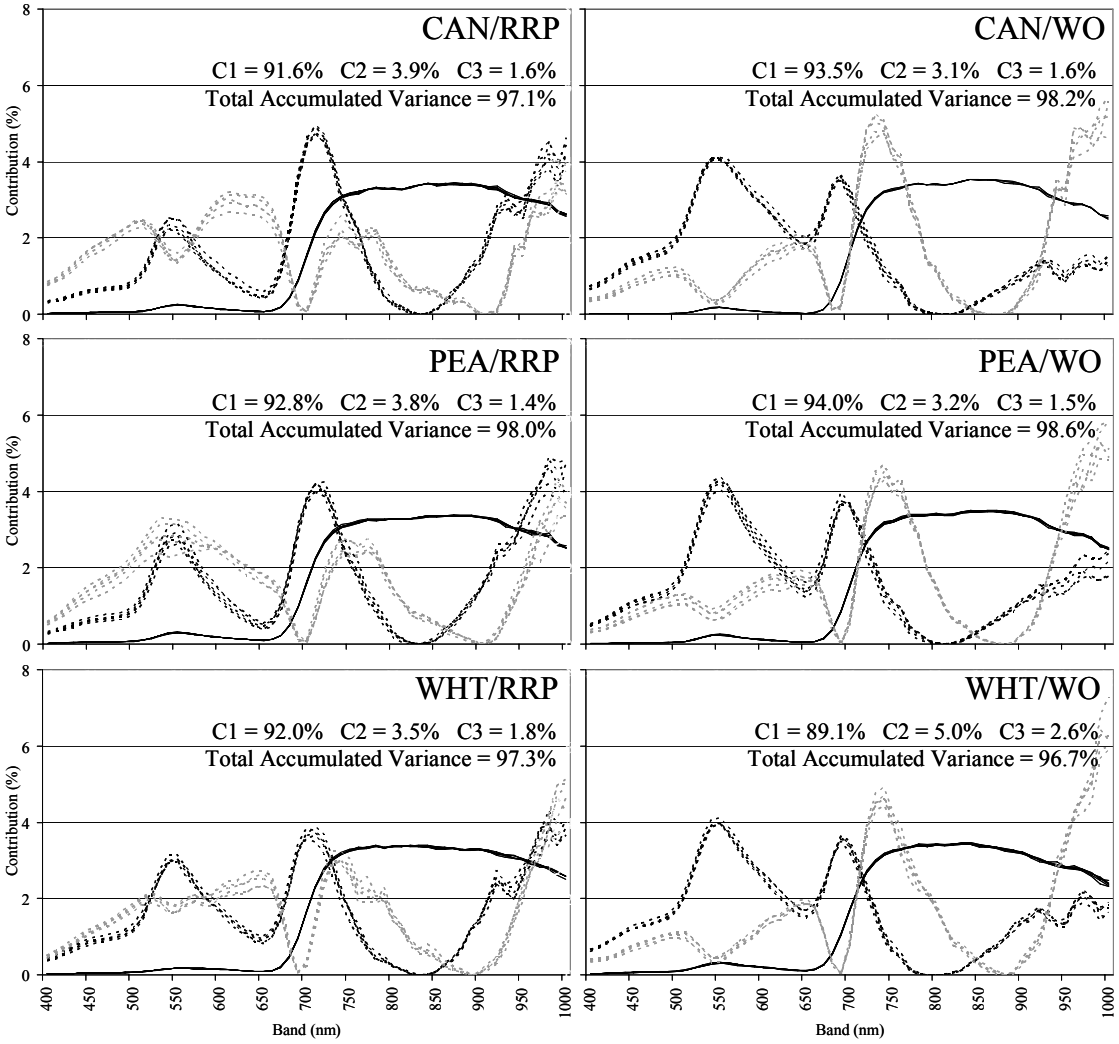

Figure 4.11 Percent contribution of original wavebands to PCA components C1 (solid black), C2 (dashed black) and C3 (dashed grey) of first 5 repetitions for crop/weed combinations on July 19 acquisition date. The % of total variance accounted for by each C (average of 5 repetitions) is shown with cumulative variance for each weed/crop combination.

Eigenvalues from these analyses showed approximately 97% of the variance in the original datasets was accounted for in the first three components. The contributions from the original wavebands were very similar among the first five repetitions, though slight differences can be observed in component 2 and to a greater extent in component 3. The first component accounted for 89-94% of the total variance in the data and was

loaded heavily in the NIR region with 720-900 nm given similar representation for all crop/weed combinations. The second component represented 3-5% of the remaining variance in the data. In all comparisons, a high contribution was observed in the green (520-570 nm), red edge (680-740 nm) and again in the NIR (900-1000 nm). The crop/WO combinations showed a slightly higher contribution (~1%) at the green peak (550 nm) compared to the crop/RRP combinations. The third component accounted for very little variance from the original dataset (1-3%), with contributions in the blue-green edge (490-510 nm), red (640-660 nm), red-edge(720-750 nm) and NIR (950-1000 nm) for all combinations except PEA/RRP. This latter crop/weed combination did not show the blue-green and red peaks but high contribution through the visible range peaking in the green (550 nm) was observed. Differences again can be seen between the RRP and WO combinations as the WO had a lower contribution in the visible range and higher contribution in the red-edge (720-750 nm), while RRP was loaded evenly and somewhat higher in the visible spectrum.

4.5.3 Waveband Selection

Through identification of discriminatory wavebands using SDA and PCA, a subset of seven wavebands was selected from the original 61. The wavebands were selected with a single multispectral (seven band) system in mind and centered at 480, 550, 600, 670, 720, 840 and 930 nm. This subset of narrow (10 nm) wavebands representing a multispectral acquisition was used as input for the reduced waveband series of classifications presented later in this chapter (Section 4.6.3).

4.6 Image Classification

Two image classification methods were tested for accuracy in defining crop and weed pixels within the acquired data. The first, MLC evaluates the feasibility of using statistical methods to separate the crop/weed spectra. The second, ANNs, which model the biological neurons in the brain, has no prior assumptions of the dataset (i.e. multivariate normality) and is suited to handle very large quantities of data efficiently (Atkinson and Tatnall, 1997). The identification of plant species within the acquired image data is a preliminary step for mapping weed locations within the field, and constitutes an essential component for implementation of site-specific herbicide management techniques.

Prior to classification, image data were segmented using MCARI thresholding (Section 4.3.1) and only pixels identified as vegetation were passed to the classification algorithm. Three series of classifications were run, which included training and validation, over a single date (Appendices B, C), multitemporal (Appendices D, E) and with a reduced subset of seven narrow wavebands representative of a multispectral acquisition.

4.6.1 Single Date Classification

Initial classifications were run with the full image dataset input to the classification algorithms. This provided a test of classification accuracy for the two methods (MLC and ANN) with a single image acquisition. Due to insufficient emergence of WO, the July 19 classification result for the CAN/WO and WHT/WO combinations are not presented. Plant growth over the 5-day period between the two imaging dates provided adequate WO samples for analysis of all weed/crop combinations on the later

date (July 26). Results from both the MLC and ANN classification validations are presented in Tables 4.1 and 4.2.

Overall accuracies of greater than 80% were obtained with the MLC except in two cases (WHT/WO and PEA/WO on July 26). This overall accuracy seems encouraging however, the Kappa coefficients indicate some problems. The highest Kappa value occurred for the July 19 PEA/RRP classification (0.82) while the Kappa values for other crop/weed combinations ranged from 0.06 to 0.65. These values indicate confusion between classes, which can be assessed through individual class omission and commission errors. The July 19 classifications provided lower errors (3-14% and 3-19% commission and omission) for the crop classes with generally higher weed class error (5 to 48%). The July 26 validation did not show the same trend as both crop and weed classes had high classification errors, especially in the crop/WO combinations. When considering overall accuracy and Kappa statistic, the best results were observed in classification of the PEA/RRP combination (for both acquisition dates), with the later date showing slightly lower class accuracy (Figure 4.12).

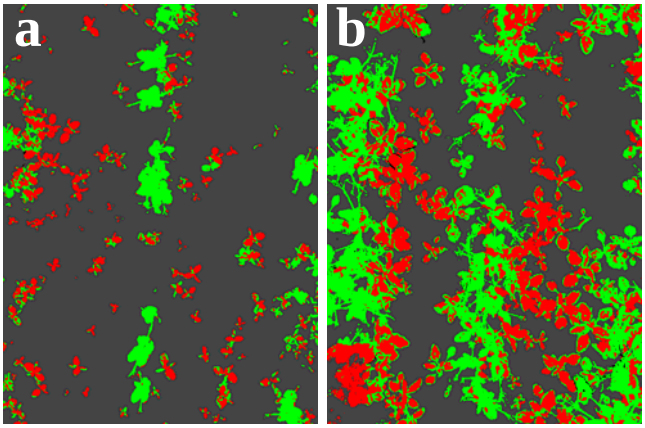

Figure 4.12 Single date MLC classification output of PEA (green) and RRP (red) on (a) July 19 and (b) July 26 image data.

Table 4.1 MLC classification accuracy assessment with 61 wavebands input to classification for (a) July 19 and (b) July 26 image acquisitions.

a	Crop Class Error		Weed Class Error		Overall	
	Commission (%)	Omission (%)	Commission (%)	Omission (%)	Accuracy (%)	Kappa
CAN/RRP	3.1	19.2	41.8	9.3	82.9	0.59
PEA/WO	2.4	5.9	47.7	32.1	91.8	0.56
WHT/RRP	14.2	4.6	12.2	35.1	85.5	0.65
PEA/RRP	12.3	3.7	4.7	15.1	90.9	0.82

b	Crop Class Error		Weed Class Error		Overall	
	Commission (%)	Omission (%)	Commission (%)	Omission (%)	Accuracy (%)	Kappa
CAN/RRP	1.4	18.8	56.0	7.7	82.6	0.49
WHT/WO	6.6	32.8	51.7	13.6	72.1	0.43
PEA/WO	4.8	49.0	88.9	29.6	52.6	0.06
WHT/RRP	26.0	38.5	14.0	8.8	82.7	0.56
CAN/WO	0.2	9.3	86.0	11.0	90.6	0.22
PEA/RRP	21.5	14.8	13.5	20.5	82.2	0.64

ANN classification accuracies were markedly improved over the MLC as can be observed from the overall accuracies and Kappa coefficients (Table 4.2 a, b). The weed class commission errors for July 19 were high (PEA/WO, CAN/RRP) but not as high as those observed in the MLC. The July 26 classifications produced less encouraging results than those obtained on July 19. The highest weed class errors occurred in commission of PEA and CAN pixels to the WO class on July 26.

Table 4.2 ANN classification accuracy assessment with 61 bands input to classification for (a) July 19 and (b) July 26 image acquisitions.

a	Crop Class Error		Weed Class Error		Overall	
	Commission (%)	Omission (%)	Commission (%)	Omission (%)	Accuracy (%)	Kappa
CAN/RRP	1.6	5.5	17.3	5.5	94.5	0.85
PEA/WO	0.7	4.4	33.2	6.7	95.4	0.75
WHT/RRP	5.8	11.0	20.8	11.5	88.8	0.75
PEA/RRP	5.4	6.0	6.7	5.9	94.0	0.88

b	Crop Class Error		Weed Class Error		Overall	
	Commission (%)	Omission (%)	Commission (%)	Omission (%)	Accuracy (%)	Kappa
CAN/RRP	1.6	6.1	31.7	10.5	93.4	0.74
WHT/WO	11.2	25.4	48.8	29.1	73.7	0.41
PEA/WO	1.4	22.5	74.7	13.1	78.2	0.30
WHT/RRP	25.1	8.2	3.6	12.4	88.8	0.74
CAN/WO	0.2	9.9	87.0	12.6	90.1	0.20
PEA/RRP	18.2	15.1	13.7	16.6	84.1	0.68

Spatially mis-classification was not random. Generally, RRP was better classified by MLC (Figure 4.13e, 4.14e) with darker/shadowed CAN and WHT pixels classified incorrectly (Figure 4.13b, 4.14b). Crop species were classified more accurately using the ANN technique as error occurred along leaf edges (Figure 4.13c) with the darker pixels in RRP being incorrectly classified (Figure 4.13f, 4.14f).

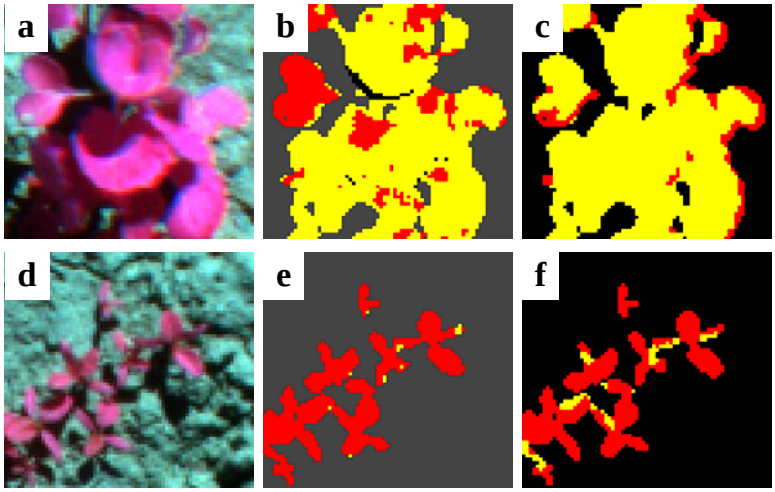

Figure 4.13 MLC (b,e) and ANN (c,f) classification output of July 19 CAN (yellow) (a,b,c)/RRP (red) (d,e,f) treatment.

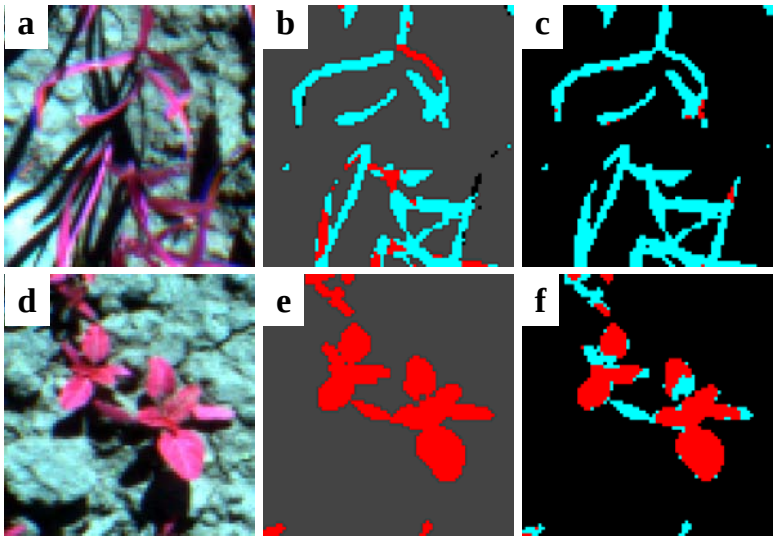

Figure 4.14 MLC (b,e) and ANN (c,f) classification output of July 19 WHT (cyan) (a,b,c)/RRP (red) (d,e,f) treatment.

Mis-classification was similar in the crop/WO classifications for both MLC and ANN techniques. WO was classed well (Figure 4.15 e and f, 4.16 e and f) with mis-classification occurring mainly with respect to PEA tendrils (Figure 4.15 b and c) and CAN petioles and leaf veins (Figure 4.16 b and c).

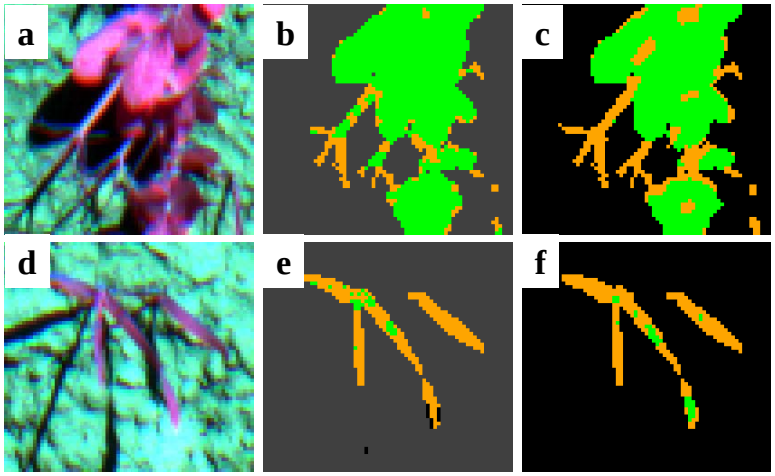

Figure 4.15 MLC (b,e) and ANN (c,f) classification output of July 19 PEA (green) (a,b,c)/WO (orange) (d,e,f) treatment.

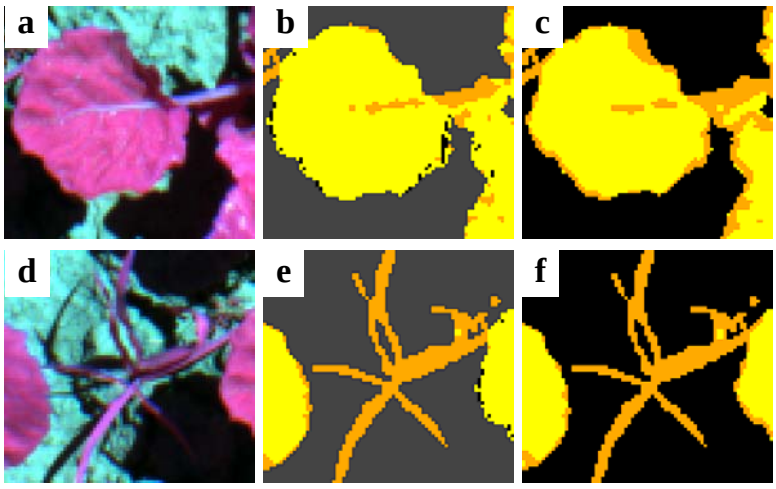

Figure 4.16 MLC (b,e) and ANN (c,f) classification output of July 26 CAN (yellow) (a,b,c)/WO (orange) (d,e,f) treatment.

Overall, the crop/RRP classifications were less prone to error than the crop/WO in both the MLC and ANN output. Higher classification accuracy was also obtained on the earlier plant stage (July 19), a trend observed with both classification methods (Tables 4.1 and 4.2).

4.6.2 Multitemporal Classification

The two dates of image acquisition provided an opportunity to evaluate the ability of the classification algorithms to account for not only spatial reflectance variation but also variability of spectral reflectance in the temporal domain. This series of classifications used both July 19 and 26 data for training of the MLC and ANNs. Once the models were built, crop/weed combinations on each date were classified.

In examining the MLC class validation (Table 4.3 a, b) the overall accuracies were again misleading as evaluation of the Kappa coefficients and class omission and commission errors indicate the classification complexity. Excluding the PEA/RRP combination, generally poor results were obtained with commission error on both July 19 (16-67%) and 26 (22-93%) and omission errors on July 19 (16-49%) being high for the weed classes. Crop omission error was also high (20-66%) for all combinations on the later acquisition date. The best results occurred with the July 19 PEA/RRP combination (91% overall and a Kappa of 0.82) followed by WHT/RRP (85% overall and a Kappa of 0.64) (Figure 4.17a, b). Similar to the single date MLC classifications, the earlier date showed higher class accuracies than those from July 26.

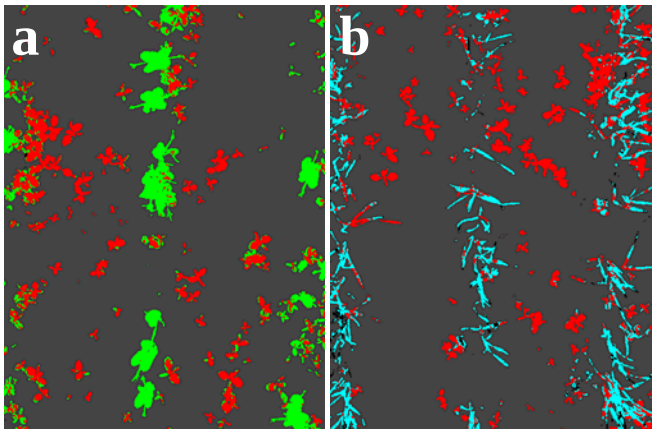

Figure 4.17 Multitemporal MLC classification output of crop (PEA=green, WHT=cyan) and weed (RRP=red) combinations acquired on July 19.

Table 4.3 Classification accuracy assessment for multitemporal classifications of MLC for (a) July 19 and (b) July 26.

a	Crop Class Error		Weed Class Error		Overall	
	Commission (%)	Omission (%)	Commission (%)	Omission (%)	Accuracy (%)	Kappa
CAN/RRP	5.4	24.0	48.5	15.7	77.8	0.48
PEA/WO	2.7	13.2	67.3	33.2	85.1	0.38
WHT/RRP	13.1	6.6	16.3	32.9	84.9	0.64
PEA/RRP	10.9	5.6	6.7	12.8	91.0	0.82

b	Crop Class Error		Weed Class Error		Overall	
	Commission (%)	Omission (%)	Commission (%)	Omission (%)	Accuracy (%)	Kappa
CAN/RRP	0.1	43.9	75.1	2.6	61.4	0.24
WHT/WO	2.9	62.0	64.8	3.2	53.2	0.22
PEA/WO	4.3	49.0	88.4	26.0	52.8	0.07
WHT/RRP	22.1	66.0	21.5	3.9	78.3	0.37
CAN/WO	0.0	21.5	92.8	1.4	78.8	0.11
PEA/RRP	16.1	19.7	16.1	13.6	83.6	0.67

Following the trend observed in the single date classifications, the ANN overall accuracies were again better (3-30%) than the MLC, with July 19 (Figure 4.18) out performing July 26. High commission errors (26-70%) were observed for both dates in the weed class with the exception of the WHT/RRP and PEA/RRP combinations. The

crop errors were low for all combinations between both dates, except for WHT/RRP which exhibited 21% and 29% commission error on July 19 and 26, respectively. The WHT/WO classifications, which proved difficult in the single date analyses, improved with the use of the ANN method and multitemporal data (85% overall and a Kappa of 0.61). As was observed with the multitemporal MLC classifications, the best results were achieved with the PEA/RRP on both dates. The crop/RRP classifications were generally better than the crop/WO combinations.

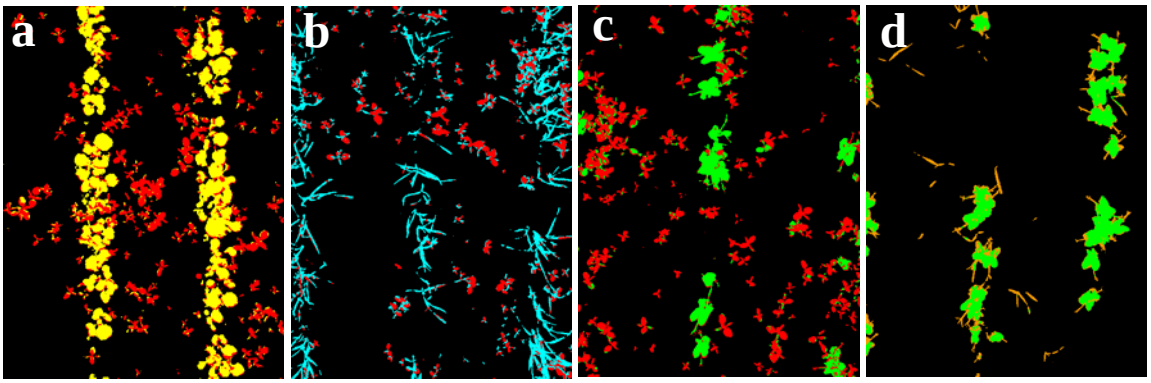

Figure 4.18 Multitemporal ANN classification output of crop (CAN=canola, PEA=green, WHT=cyan) and weed (RRP=red, WO=orange) combinations acquired on July 19.

Table 4.4 Classification accuracy assessment for ANNs multitemporal classifications for (a) July 19 and (b) July 26.

a	Crop Class Error		Weed Class Error		Overall	
	Commission (%)	Omission (%)	Commission (%)	Omission (%)	Accuracy (%)	Kappa
CAN/RRP	2.8	8.6	25.5	9.7	91.2	0.76
PEA/WO	0.4	10.2	52.8	4.1	90.3	0.58
WHT/RRP	21.2	14.0	7.0	11.0	88.0	0.73
PEA/RRP	9.4	8.3	9.3	10.6	90.6	0.81
b	**Crop Class Error**		**Weed Class Error**		**Overall**	
	Commission (%)	Omission (%)	Commission (%)	Omission (%)	Accuracy (%)	Kappa
CAN/RRP	2.1	8.4	40.0	13.4	90.9	0.66
WHT/WO	8.7	11.6	27.6	26.5	84.6	0.61
PEA/WO	2.7	15.2	70.4	27.6	83.8	0.34
WHT/RRP	29.5	9.9	4.5	15.2	86.4	0.69
CAN/WO	0.5	7.6	85.7	24.9	92.1	0.22
PEA/RRP	11.7	15.4	13.0	9.9	87.5	0.74

4.6.3 Reduced Waveband Classification

Because multispectral data are less costly to acquire and can be processed more efficiently, a final series of classifications examined the need for hyperspectral image data as opposed to a smaller subset of wavebands. Evaluation of the information content of each waveband (PCA) as well as the discriminatory power (SDA) from each provided an opportunity to reduce spectral dimensionality used in this classification series (Section 4.5). This reduced set of wavebands (480, 550, 600, 670, 720, 840 and 930 nm) were used to classify the July 19 acquisitions (Figure 4.19).

Similar results were obtained for both MLC and ANN classification techniques with the latter showing a slight (1-3%) improvement in overall accuracy (Table 4.5 a, b). Continuing the trend observed in the previous series of classifications, the highest accuracies were obtained with the PEA/RRP combination (92%) and the commission error for weed classes were generally high for both MLC (8-47%) and ANNs (6-41%).

The reduction of information input to the classification algorithms produced an improvement in MLC accuracy of CAN/RRP (9% overall and 0.18 Kappa) with a decrease of 1-2% in overall accuracy in the other crop/weed combinations. Using ANNs, the full hyperspectral dataset provided 1-2% higher overall classification accuracy. Generally, the reduction of the original 61 wavebands to 7 provided similar classification results (spatially and contingency tables) in crop/weed combinations.

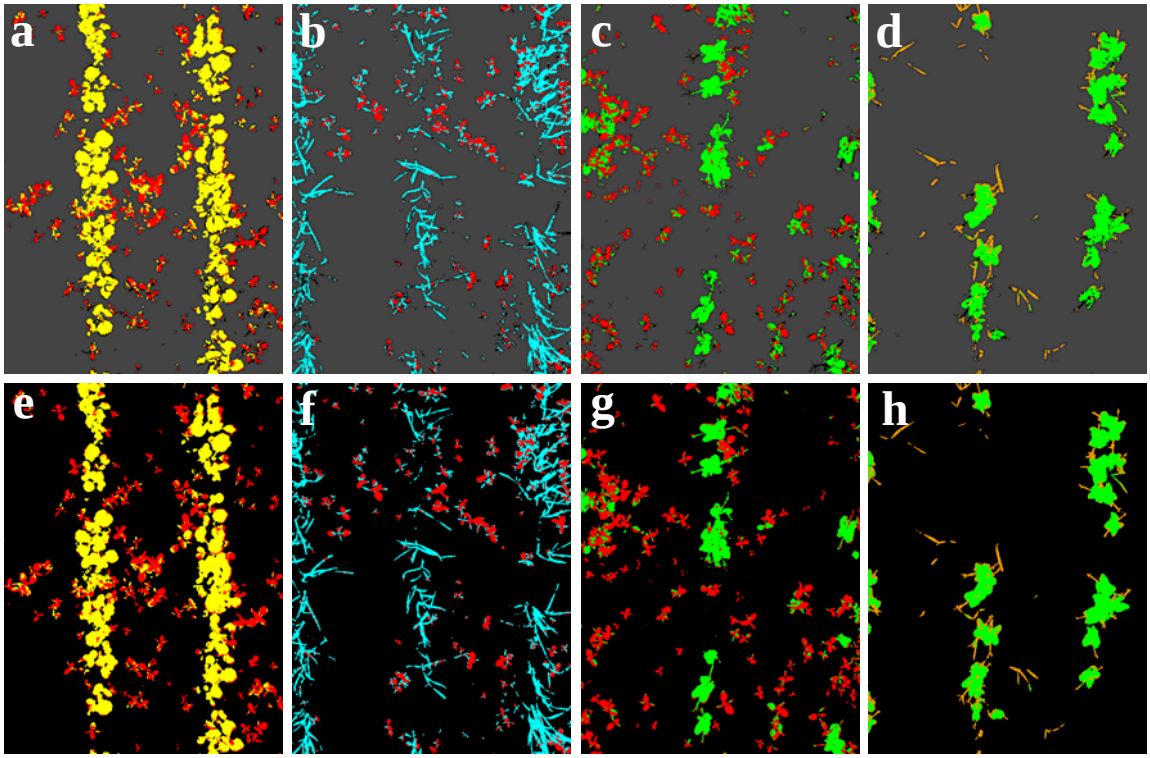

Figure 4.19 MLC (a,b,c,d) and ANN (e,f,g,h) reduced waveband classification output of crop (CAN=yellow, WHT=cyan, PEA=green) and weed (RRP=red, WO=orange) combinations acquired on July 19, 2005.

Table 4.5 Crop/weed (July 19 only) classification accuracy assessment for the reduced set of wavebands input to (a) MLC and (b) ANN algorithms.

a	**Crop Class Error**		**Weed Class Error**		**Overall**	
	Commission (%)	**Omission (%)**	**Commission (%)**	**Omission (%)**	**Accuracy (%)**	**Kappa**
CAN/RRP	2.7	7.1	16.2	11.7	91.9	0.78
PEA/WO	0.9	9.6	46.9	13.8	90.1	0.56
WHT/RRP	5.3	15.2	22.0	15.5	84.7	0.68
PEA/RRP	8.9	10.0	7.5	11.7	89.2	0.79
b	**Crop Class Error**		**Weed Class Error**		**Overall**	
	Commission (%)	**Omission (%)**	**Commission (%)**	**Omission (%)**	**Accuracy (%)**	**Kappa**
CAN/RRP	2.9	7.2	22.5	10.1	92.2	0.78
PEA/WO	0.9	6.1	41.3	8.6	93.7	0.68
WHT/RRP	21.9	12.8	6.4	11.6	88.0	0.73
PEA/RRP	8.8	6.6	7.5	10.0	91.8	0.84

CHAPTER 5 DISCUSSION AND CONCLUSIONS

5.1 Introduction

The following section discusses results obtained through segmentation procedures, single date, reduced band and multitemporal classification series. The implications of these findings in relation to SSHM techniques are presented. Finally a summary of this study, with major findings and future research directions, concludes the chapter.

5.2 Segmentation

Segmentation of ground-based image data prior to classification is an efficient means of simplifying the classification problem. Through the prior elimination of background pixels, only foreground classes need be identified. This effectively reduces the number of classes required for image generalization and in turn, simplifies the complexity of the classification problem. Elimination of background pixels also increases processing efficiency, especially in cases where vegetated ground cover is low, as only pixels of interest require further analysis.

Thresholding of the transformed hue colour component provided an initial test for separating vegetated pixels in laboratory acquired image data. This procedure, found to be robust in defining vegetated pixels with varied illumination conditions, has proven useful in many studies involving RGB colour image data (Cheng et al., 2001; Burks et al., 2000b, 2005). The processing involved in this method (colour transformation, threshold and post-morphological operator application) may be limiting in real-time applications where computational efficiency is key to successful operation. Extension of

reflectance measurement into the NIR region of the EM spectrum (through hyperspectral image acquisition) provided an opportunity to utilize specific vegetation indices in the threshold-based segmentation. The selected VI (MCARI) was designed to be responsive to both chlorophyll variation and resistant to non-photosynthetic material effects (Daughtry et al., 2000; Haboudane et al., 2002). The spectral reflectance in the MCARI wavelength regions (560, 670 and 700 nm) were different between vegetation (foreground) and soil or litter (background), providing separation in spectral space, which lends itself well to segmentation by threshold techniques. This MCARI threshold procedure may be more computationally efficient than hue transformation thresholding as only two procedures (MCARI calculation and thresholding) were required to identify a vegetation pixel in the image data. No post-filtering was required to eliminate spurious pixels in the threshold output. The MCARI method also provided consistent results in defining leaf matter under full sun or shaded scenarios and thus is deemed very useful in defining pixels of vegetation from high spatial resolution image data.

Watershed segmentation provided an opportunity for identification of not only vegetated pixels in acquired image data, but also aggregation of these pixels into individual leaf segments. This definition of leaf segments is the first step in utilizing structural/shape characteristics for discrimination between species. The watershed segmentation was not able to define individual plant leaves. The high variability of pixel values caused extensive over-segmentation using the 255 grey-level hue colour component. Over-segmentation was reduced through quantizing the data range of pixel values but still did not provide a consistent method for segmenting individual leaves. Since these initial tests on laboratory image data provided less than encouraging results,

especially in terms of automated leaf segment detection, further evaluation of this algorithm was not undertaken.

Image segmentation methods for extraction of leaf shape and species identification based on spatial characteristics were hindered by variability in leaf illumination and leaf occlusion as species ground cover increased. These limitations were similar to those found by others in leaf shape measurement research (Chapron et al., 1999; Cheng et al., 2001; Brown and Noble, 2005). Since leaf shape could not be extracted consistently with automated methods, focus shifted to pixel-based classification using spectral reflectance characteristics. Though individual leaves could not be segmented, benefits of using an initial segmentation for defining vegetated pixels were two-fold. Image classification was simplified through elimination of background classes (soil and litter) and image processing efficiency was increased, as only pixels of interest were passed to the classification procedure.

5.3 Image Statistics

The very high spatial resolution of the acquired image data was beneficial in identifying pure vegetated pixels and reduced the possibility for mixed targets (vegetation and background) in a single pixel. The observed variability in spectral reflectance is inherent to high spatial resolution image data due to bi-directional reflectance effects. In lower resolution data, the variability is "diluted out" of the pixel values and as spatial resolution increases, greater variability exists in the data with finer target features being resolved. This variability of reflectance targets of the same class may cause problems in separation of crop/weed mixtures based on spectral characteristics.

Through comparison of reflectance values on both field acquisition dates, reflectance characteristics of the selected species changed in the six day span between measurements. This reinforces the importance of timely (at specific plant stages) remotely sensed data collection if crop/weed discrimination is to be successful.

Analysis of differences between crop and weed species spectra identified several trends that can be attributed to differences in leaf internal structure (monotcotyledon and dicotyledon). In the WHT/WO comparison, there was no reflectance difference observed in the NIR region, a region in which reflectance characteristics are mainly affected by leaf structural (morphological) components including protein, starch and oils (Curran, 1989).

In a comparison of the dicotyledon crops (CAN, PEA) with the monocotyledon weed species (WO), reflectance differed in all wavebands from the red edge (700-780 nm) and NIR (790-1000 nm). The NIR portion of the EM spectrum reflected can be defined as a key wavelength range for defining plant species with differences in leaf structure, as was observed between monocotyledon and dicotyledon species. Basic descriptive statistics such as image mean and standard deviation characterized some differences between species, but definitive conclusions were hindered by overall data variance. Statistical analyses including ANOVA, PCA and SDA provided a means of defining specific wavelengths of importance for species discrimination.

Several studies have identified important wavebands for spectral characterization of plant species. Lewis (2002) conducted a study for characterization of arid zone plants in Australia; identifying wavebands centered at 420, 460, 545, 550, 555, 580, 704, 710, 760, 780, 800, 850, 900 nm to be the most important for discrimination. More recently,

12 hyperspectral bands (centered at 495, 525, 550, 568, 668, 682, 696, 720, 845, 920, 982, 1025 nm) were identified as important for agricultural crop/crop discrimination studies (Thenkabail et al., 2004).

Through PCA, several important spectral regions were identified, the most important being the NIR, as was observed in the descriptive statistics. Secondly, the blue-green, green and red edge regions contained discriminatory information for crop/weed species. A slightly different contribution was observed (~1 %) between RRP and WO combinations, particularly in the red-edge region, which may again be attributed to differences in leaf structure (monocotyledon or dicotyledon). This analysis identified specific areas of the EM spectrum (480-500, 550, 600-670, 720-750 and 760-1000 nm) that were used in construction of resultant components. These spectral regions correspond to past studies conducted by Lewis (2002) and Thenkabail et al. (2004).

A second analysis (SDA) was used for identification of specific narrow wavebands from the hyperspectral dataset with significant reflectance differences between species. Trends were observed that can be attributed to leaf structural characteristics as the comparison of dicotyledon (CAN/RRP, PEA/RRP) species tended to shift importance with selected wavebands occurring in the visible range. The NIR region of the EM spectrum was more important than the visible portion for dicotyledon and monocotyledon (CAN/WO, PEA/WO) combinations. This result was consistent with observed trends from PCA and ANOVA and suggests that the full hyperspectral dataset may not be needed to spectrally discriminate these species. To this end, through review of past studies as well as statistical analyses conducted, a selection of specific wavebands from the original image data was identified.

In selection of a reduced set of bands for this study, an important aspect to consider was the utility of these results for the end user. Since hyperspectral ground-based remote sensing systems are costly and as yet not readily available, a theoretical limit to the number of wavelengths was set. To test the efficiency of this theoretical multispectral sensor, a single set of bands were tested for discrimination of all crop and weed combinations, in essence providing a sensor-specific evaluation across the different classification problems. The wavebands, selected with primary importance given to PCA and SDA results and coincident to past studies (Lewis, 2002; Thenkabail et al., 2004), were centered at 480, 550, 600, 670, 720, 840 and 930 nm (10 nm bandwidth). This subset, representative of data from a multispectral system, provided the opportunity to evaluate the benefits of spectral dimensionality input to classification algorithms for species discrimination.

5.4 Classification

Several series of classifications were evaluated for discriminating between single weed/crop combinations. These included classification of image data trained over a single date, over multiple dates and with a reduced number of bands identified as being important through PCA and SDA techniques.

The single date series of classifications set a baseline evaluation of the capability of MLC and ANN algorithms to address the species discrimination problem when only a single image is acquired, and from class validation this initial test provided relatively encouraging results. The multitemporal classifications enabled assessment of weed and crop discrimination, accounting for not only spatial reflectance variation but also variation in reflectance characteristics over time. This procedure would lend itself better

to real world or end-use application as training data for these methods, which account for spectral variation over the optimal herbicide application periods, could be built into the processing procedure. Higher class accuracies were observed with multitemporally trained ANNs (84-92%), with improvements in accuracies up to 13% (July 19) and 31% (July 26) compared to MLC. MLC was hindered somewhat by the addition of the second date and was not well suited to this type of application.

Classification with a reduced set of bands enabled assessment of a multispectral camera system to discriminate between crop and weed species. Classification results were again encouraging as accuracies observed with ANNs were similar to those obtained with the full hyperspectral dataset, with a reduction in classification accuracy of only 1-2% with seven wavebands. The reduction of band dimensionality improved MLC CAN/RRP classification accuracy by 9% and generally improved crop commission and weed class omission errors. This could be attributed to the fact that statistical classifiers have potential for "confusion" if highly correlated data are used to train the classification procedure (Lillisand and Kiefer, 1987). Reduction of spectral dimensionality eliminated duplicate or similar information presented to the classifiers and resulted in a general improvement of the MLC output. The single and multitemporal date ANN model development involved assessment of all input bands for information content and a reduced number of bands were selected in the software from the 61 band input set. Using a reduced set of bands deemed important in PCA and SDA, rather than letting the software select its own, may not have been the best procedure for spectral dimensionality reduction in the network models. Even with these very few wavebands selected (seven), classification accuracy differences (61 vs 7 bands) in the ANN models was very small (1-

2%). This effect on class accuracy was negligible and attention must be given to the cost savings of multispectral over hyperspectral data acquisition as well as potential computational efficiency gains. MLC and to a lesser extent ANN classification using fewer bands will result in less computational overhead (Lillisand and Kiefer, 1987) which is important when envisioning end-use procedures applied to a real-time herbicide application system.

The overall accuracies obtained for the different crop/weed combinations were encouraging, especially in terms of classifying RRP in the different crops. The PEA/RRP combination was consistently well classified (> 82%) through all series of classifications and suggested that these two species are easily separated in the spectral domain. Unfortunately, classifying WO in the selected crops was difficult as can be observed in lower Kappa coefficients. Throughout most classification series the commission error was highest compared to other class error types (weed omission and crop commission/omission). Commission error represents pixels belonging to the crop class being labelled as weeds. In terms of site-specific herbicide application systems, this type of error would result in more herbicide being applied than was actually needed. The reverse case (weeds mis-labelled as crop) could be considerably more troublesome as this would result in missed herbicide applications and potential loss in yield due to continued weed competition. The error of commission may be considered the less severe because the cost of extra herbicide would overcome the loss of yield in the reverse scenario.

Spatially the classification error did not appear to be random and trends emerged as the two classification techniques used seemed to favour specific classes. MLC consistently classified the RRP well with error typically occurring in dark/shadowed crop

pixels. ANN generally classified the crop species better than MLC with classification error occurring in weed pixels at the upper and lower end (shadow) of reflectance value range. Both techniques provided similar results in classification of the CAN/WO and PEA/WO combinations.

From the validated classification results it can be stated that the ANN classification models out performed the MLC. Furthermore, these models are much more efficient in terms of computational overhead than statistical classifiers. This suggests that ANN classification techniques are better suited to real-time SSHM.

5.5 Site Specific Herbicide Management

Seeding crop/weed combinations to field plots with image acquisition in-field resembles image data that could be collected in a SSHM system. Detection and mapping of weed species in-field without artificial lighting increases classification complexity due to variable illumination conditions. Through selection of supervised classification methods which can be trained to account for this variability, identification of certain crop and weed species can be obtained with considerable accuracy (> 83%). The examination of plant stage effects on spectral reflectance is another critical factor for implementation of SSHM. In order to detect weed species, the temporal reflectance variability in plant species must be characterized and trained into the classification method. Potential exists for classification algorithms to be trained over multiple dates, with this investigation showing that species differentiation is possible if training data can encompass the complete variability of spectral reflectance throughout the optimal herbicide application timeframe.

The availability of ground-based hyperspectral image data provided a means for evaluation of not only high spectral, but also very high spatial information. This hyperspectral system is not proposed as being applied directly to a SSHM system but rather as a useful research tool, providing substantial information in the image data acquired. The initial band reduction results show a negligible difference in classification accuracy when a subset of the total hyperspectral data cube is classified. The reduction of bands and subsequent classification suggests a multispectral sensor would provide similar classification accuracies and therefore a full hyperspectral dataset is not necessarily required for crop/weed discrimination.

5.6 Conclusions

This study, which investigated species reflectance differences, segmentation, and image classification techniques for discrimination of field grown crop/weed species combinations, shows potential for the use of remotely sensed data for high resolution herbicide prescription maps. Classification of these image data provides a means of mapping weed location and density within a field, an integral step in successful application of SSHM techniques.

Segmentation of foreground and background pixels from imagery was presented as an initial step in eliminating background pixels and in turn classifying only pixels of interest. Through visual analysis, the MCARI showed excellent results in terms of consistency in identification of vegetated pixels.

Classification using MLC and ANNs proved useful for discrimination of single weed/crop mixtures over both image acquisition dates. Generally the crop/RRP combinations achieved higher accuracies than the crop/WO with best results obtained in

classification of the PEA/RRP combination. The earlier plant stage (July 19) showed consistently better classification results than the latter July 26 acquisition, suggesting that optimal species discrimination can be obtained at early plant growth stages. Since observed reflectance characteristics varied as a function of plant stage, both classification techniques were evaluated for their ability to account for temporal variability. ANN models, with their efficiency in handling complex feature space, provided better results than MLC in the multitemporal series of classifications. Therefore creation of a single classification model trained to encompass the variability of spectral reflectance throughout the optimal herbicide application timeframe is possible.

The identification of important spectral bands for species discrimination was achieved through PCA and SDA with seven wavebands selected from the original 61 waveband dataset. This waveband reduction slightly lowered ANN overall accuracies (less than 3%), with most crop/weed combinations and suggested that a seven band multispectral sensor may be adequate in discrimination between two plant species.

5.7 Future Research

Very high resolution image data can be prone to spectral variability caused by leaf angle and orientation effects as well as atmospheric illumination changes. In this study, image data were collected only on clear sunny days through hours of peak incoming solar radiation to reduce the radiation variability. Typical application of herbicides to agricultural systems would be throughout the entire day and would require constant calibration for accurate reflectance measurements throughout this period. Further research must focus on effects of differential illumination conditions as well as maintaining consistency in the image data acquired. The possibility of multiple weeds

growing within the same field was also an issue that was not examined and further study is required to address this scenario which represents real-world application of SSHM techniques.

The movement towards successful application of SSHM techniques will only be achieved through investigation of new emergent technologies. Though these technologies are by no means cost effective for direct SSHM implementation, new procedures and evaluation of these advancements is essential to SSHM development. Investigation into species discrimination and application of remotely sensed data for mapping weed location and density today, leads to end-use application tomorrow. As imaging systems and processing technology become more widely available and cost effective with proven research behind them, acceptance and implementation will surely follow.

REFERENCES CITED

Aitkenhead, M.J., Dalgetty, I.A., Mullins, C.E., McDonald, A.J.S., and Strachan, N.J.S. (2003) Weed and crop discrimination using image analysis and artifical intelligence methods. *Computers and Electronics in Agriculture*, 39: 157-171.

Atkinson, P.M., and Tatnall, A.R.L. (1997) Neural networks in remote sensing. *International Journal of Remote Sensing*, 18(4): 699-709.

Bechdol, M.A., Gualtieri, J.A., Hunt, J.T., Chettri, S., and Garegnani, J. (2000) Hyperspectral imaging: a potential tool for improving weed and herbicide management. In *Proc. 5th Int. Conference on Precision Agriculture*, Bloomington, Minnesota, 16-19 July 2000.

Benediktsson, J.A., Swain, P.H. and Ersoy, O.K. (1990) Neural network approaches versus statistical methods in classification of multisource remote sensing data. *IEEE Transactions on Geoscience and Remote Sensing*, 28:540-552.

Beucher, S. (1992) The watershed transformation applied to image segmentation. In *10th Pfefferkorn Conference on Signal and Image Processing in Microscopy and Microanalysis*, Cambridge, UK, 16-19 September, 1991.

Beucher, S., and Lantuejoul, C. (1979) Use of watersheds in contour detection. In *Proceedings International Workshop on Image Processing, Real-time Edge and Motion Detection/Estimation*, CCETT/IRISA, France, pp. 180-186.

Bleau, A., and Leon, L.J. (2000) Watershed-based segmentation and region merging. *Computer Vision and Image Understanding*, 77: 317-370.

Borregaard, T., Neilsen, H., Norgaard, L., and Have, H. (2000) Crop-weed discrimination by line imaging spectroscopy. *Journal of Agricultural Engineering Research*, 75: 389-400.

Brown, R.B., and Noble, S.D. (2005) Site-specific weed management: sensing requirements-what do we need to see? *Weed Science*, 53: 252-258.

Brown, R.B., and Steckler, J.-P.G.A. (1993) Weed patch identification in no till corn using digital imagery. *Canadian Journal of Remote Sensing*, 19(1): 88-91.

Brown, R.B., and Steckler, J.-P.G.A. (1995) Prescription maps for spatially variable herbicide application in no-till corn. *Transactions of the ASAE*, 38(6): 1659-1666.

Brown, R.B., Steckler, J.-P.G.A., and Anderson, G.W. (1994) Remote sensing for identification of weeds in no-till corn. *Transactions of the ASAE*, 37(1): 297-302.

Brown, R.J., Staenz, K., McNairn, H., Hopp, B., and Van Acker, R. (1997) Application of high resolution optical imagery to precision agriculture. *International Symposium, Geomatics in the Era of RADARSAT (GER'97)*, Ottawa, Canada, 25-30 May, 1997, pp. 9.

Burks, T.F., Shearer, S.A., Gates, R.S., and Donohue, K.D. (2000b) Backpropagation neural network design and evaluation for classifying weed species using color image texture. *Transactions of the ASAE*, 43(4): 1029-1037.

Burks, T.F., Shearer, S.A., Heath, J.R., and Donohue, K.D. (2005) Evaluation of neural-network classifiers for weed species discrimination. *Biosystems Engineering*, 91(3): 293-304.

Burks, T.F., Shearer, S.A., and Payne, F.A. (2000a) Classification of weed species using color texture features and discriminant analysis. *Transactions of the ASAE,* 43(2): 441-448.

Carter, G.A. (1991) Primary and secondary effects of water content on the spectral reflectance of leaves. *American Journal of Botany,* 78(7): 916-924.

Chapron, M., Requena-Esteso, M., Boissard, P., and Assemat, L. (1999) A method for recognizing vegetal species from multispectral images. In: *Precision Agriculture 1999 2nd European Conference on Precision Agriculture* (JV Stafford, Ed.), Sheffield Academic Press, Sheffield, UK. pp. 239-248.

Cheng, H.D., Jiang, X.H., Sun, Y., and Wang, J. (2001) Color image segmentation: advances and prospects. *Pattern Recognition*, 34: 2259-2281.

Cho, S.I., Lee, D.S., and Jeong, J.Y. (2002) Weed-plant discrimination by machine vision and artificial neural network. *Biosystems Engineering*, 83(3): 275-280.

Crop Life (2007) Annual Report 2005/2006. Website: http://www.croplife.ca/english/pdf/annnualreport/annualreport05-6-eng.pdf, Accessed April 4, 2007.

Curran, P.J. (1989) Remote sensing of foliar chemistry. *Remote Sensing of Environment,* 30: 271-278.

Daughtry, C.S.T., Walthall, C.L., Kim, M.S., Brown de Colstoun, E., and McMurtrey, J.E. (2000) Estimating corn leaf chlorophyll concentration from leaf canopy reflectance. *Remote Sensing of Environment*, 74: 229-239.

Edmund Optics (2007) Online Catalogue 2007. Website: http://edmundoptics.com/onlineCatalog/displayproduct.cfm?productID=1615, Accessed May 29, 2007.

El-Faki, M.S., Zhang, N., and Peterson, D.E. (2000a) Factors affecting color-based weed detection. *Transactions of the ASAE*, 43(4): 1001-1009.

El-Faki, M.S., Zhang, N., and Peterson, D.E. (2000b) Weed detection using color machine vision. *Transactions of the ASAE*, 43(6): 1969-1978.

Foley, J.D. and Van Dam A. (1982) *Fundamentals of interactive computer graphics*. Addison-Wesley Longman Publishing Co. Inc., Boston, Massachusetts.

Gausman, H.W., Allen, W.A., Weigland, C.L., Escobar, D.E., and Richardson, A.J. (1973) The leaf mesophylls of twenty crops, their light spectra, and optical and geometrical parameters. *USDA Technical Bulletin No. 1465*, U.S. Government Printing office, Washington, D.C.

Grant, L. (1987) Diffuse and specular characteristics of leaf reflectance. *Remote Sensing of Environment*, 22: 309-322.

Haboudane, D., Miller, J.R., Tremblay, N., Zarco-Tejada, P.J., and Dextraze, L. (2002) Integrated narrow-band vegetation indices for prediction of crop chlorophyll content for application to precision agriculture. *Remote Sensing of Environment*, 81: 416-426.

Haralick, R.M., Sternberg, S.R., and Zhuang, X. (1987) Image analysis using mathematical morphology. *IEEE Transactions on Pattern Analysis and Machine Intelligence*, PAMI-9(4): 532-550.

Jensen, J.R. (1996) *Introductory Digital Image Processing; A Remote Sensing Pertspective.* (K.C. Clarke Ed.), Prentice-Hall, Inc, Upper Saddle River, New Jersey.

Kanellopoulos, I., and Wilkinson, G.G. (1997) Strategies and best practice for neural network image classification. *International Journal of Remote Sensing*, 18(4): 711-725.

Kavdir, I. (2004) Discrimination of sunflower, weed and soil by artificial neural networks. *Computers and Electronics in Agriculture*, 44: 153-160.

Key, J., Maslanic, A. and Schweiger, A.J., (1989) Classification of merged AVHRR and SMMR arctic data with neural networks. *Photogrammetric Engineering and Remote Sensing*, 55: 1331-1338.

Lamb, D.W. (2000) The use of qualitative airborne multispectral imaging for managing agricultural crops – a case study in south-eastern Australia. *Australian Journal of Experimental Agriclture*, 40: 725-738.

Lamb, D.W, and Brown, R.B. (2001) Remote-sensing and mapping of weeds in crops. *Journal of Agricultural Engineering Research,* 78(2): 117-125.

Lamb, D.W., and Weedon, M.M. (1998) Evaluating the accuracy of mapping weeds in fallow fields using airborne digital imaging: *Panicum effusum* in oilseed rape stubble. *Weed Research*, 38: 443-451.

Lamb, D.W., Weedon, M.M., and Rew, L.J. (1999) Evaluating the accuracy of mapping weeds in seedling crops using airborne digital imaging: *Avena* spp. in seedling triticale. *Weed Research*, 39: 481-492.

Lawrence, J. (1994) *Neural networks: design, theory and applications*. (S. Luedeking and J. Fredrickson, Eds.), California Scientific Software, Nevada City, California.

Lewis, M. (2002) Spectral characterization of Australian arid zone plants. *Canadian Journal of Remote Sensing*, 28(2): 219-230.

Li, W., Benie, G.B., He, D., Wang, S., Ziou, D., and Gwyn, Q.H.J. (1999) Watershed-based hierarchical SAR image segmentation. *International Journal of Remote Sensing*, 20: 3377-3390.

Lillesand, T.M., and Kiefer, R.W. (1987) *Remote sensing and image interpretation*. John Wiley and Sons, New York, New York.

Lindquist, J.L., Dieleman, J.A., Mortensen, D.A., Johnson, G.A., and Wyse-Pester D.Y. (1998) Economic importance of managing spatially heterogeneous weed populations. *Weed Technology*, 12: 7-13.

Lippert, R.M., and Wolak, F.J. (1999) Weed mapping and assessment of broadcast vs. spot treatment of sicklepod weeds in soybeans. *2nd European Conference on Precision Agriculture*, Odense, Denmark, 11-15 July, 1999.

Martin-Chefson, L., Chapron, M., and Philipp, S. (1999) A two dimensional method for recognising weeds from multi-band image processing. In: *Precision Agriculture 1999 2nd European Conference on Precision Agriculture* (J.V. Stafford, Ed.), Sheffield Academic Press, Sheffield, UK. pp. 473-483.

Medlin, C.R., Shaw, D.R., Gerard, P.D., and LaMastus, F.E. (2000) Using remote sensing to detect weed infestations in *Glycine max*. *Weed Science*, 48: 393-398.

Moshou, D., Vrindts, E., De Detelaere, B., De Baerdemaeker, J., and Ramon, H. (2001) A neural network based plant classifier. *Computers and Electronics in Agriculture*, 31: 5-16.

Mortensen, D.A., Johnson, G.A., Wyse, D.Y., and Martin, A.R. (1995) Managing spatially variable weed populations. In *Site-Specific Management for Agricultural Systems*, (P. Robert, R.H. Rust, and W.E. Larson ,Eds), ASA, CSSA, SSSA, Madison, WI. pp. 398-415.

Mulla, D.J., and Schepers, J.S. (1997) Key processes and properties for site-specific soil and crop management. In *Site-Specific Management for Agricultural Systems*, (P. Robert, R.H. Rust, and W.E. Larson ,Eds), ASA, CSSA, SSSA, Madison, WI. pp. 1-18.

Noble, S.D., Brown, R.B., and Crowe, T.G. (2002) The use of spectral properties for weed detection and identification – A review. Presented at *AIC 2002 Meeting, CSAR/SCGR Program*, Saskatoon, Saskatchewan. Paper No. 02-208.

Noble, S.D., and Crowe, T.G. (2005) Analysis of crop and weed leaf diffuse reflectance spectra. *Transactions of the ASAE*, 48(6): 2379-2387.

Radhakrishnan, R., Teasdale, J.R., Liang, S., and Shuey, C.J. (2002) Remote sensing of weed canopies. In *Laboratory Spectroscopy to Remotely Sensor Spectra of Terrestrial Ecosystems* (R.S Muttiah, Ed.), Kluwer Academic Publishers, Netherlands. pp. 175-202.

Rambabu, C., Chakrabarti, I., and Mahanta, A. (2004) Flooding-based watershed algorithm and its prototype hardware architecture. *IEE Proceedings of Vision, Image & Signal Processing*, 151(3): 224-234.

Rosenblatt, F. (1958) The perceptron: a probabilistic model for information storage and organization in the brain. *Psychological Review*, 65:386-408.

Rosin, P.L. (2003) Measuring shape: ellipticity, rectangularity, and triangularity. *Machine Vision and Applications*, 14: 172-184.

Ruberto, C.D., Dempster, A., Kahn, S., and Jarra, B. (2002) Analysis of infected blood cell images using morphological operators. *Image and Vision Computing*, 20: 133-146.

Soille, P. (2000) Morphological image analysis applied to crop field mapping. *Image and Vision Computing*, 18: 1025-1032.

Smith, A.M., and Blackshaw, R.E. (2003) Weed-crop discrimination using remote sensing: a detached leaf experiment. *Weed Technology*, 17: 811-820.

Smith, M., (1993) *Neural networks for statistical modeling*. Van Nostrand Reinhold, New York, New York.

Swinton, S.M. (2005) Economics of site-specific weed management. *Weed Science*, 53: 259-263.

Tang, L., Steward, B.L., and Tian, L.F. (1999) Experimental study of a machine vision-based real-time weed sensing patch-sprayer. *Society of Automotive Engineers*. Paper No. 99F-38(UIUC-ENG-99-7009).

Tang.L., Tian, L.F., and Steward, B.L. (2000) Color image segmentation with genetic algorithm for in-field weed sensing. *Transactions of the ASAE.* 43(4): 1019-1027.

Thenkabail, P.S., Enclona, E.A., Ashton, M.S., and Van Der Meer, B. (2004) Accuracy assessments of hyperspectral waveband performance for vegetation analysis applications. *Remote Sensing of Environment*, 91: 354-376.

Thompson, J.F., Stafford, J.V., and Miller P.C.H. (1991) Potential for automatic weed detection and selective herbicide application. *Crop Protection*, 10: 254-259.

Tian, L., Reid, J.F., and Hummel, J. (1999) Development of a precision sprayer for site-specific weed management. *Transactions of the ASAE,* 42(4): 893-900.

Vincent, L., and Soille, P. (1991) Watersheds in digital spaces: An efficient algorithm based on immersion simulations. *IEEE Transactions on Pattern Analysis and Machine Intelligence*, 13(6): 583-598.

Vrindts, E., DeBaerdemaeker, J., and Ramon, H. (1999) Weed detection using canopy reflectance. In: *Precision Agriculture 1999 2nd European Conference on Precision Agriculture* (JV Stafford, Ed.), Sheffield Academic Press, Sheffield, UK. pp. 257-264.

Vrindts, E., DeBaerdemaeker, J., and Ramon, H. (2002) Weed detection using canopy reflection. *Precision Agriculture.* 3: 63-80.

Yang, C-C., Prasher, S., and Landry, J. (1998) Application of artificial neural networks to image recognition in precision agriculture. *ASAE* paper No. 98-3039.

Yang, C-C., Prasher, S., Landry, J-A., Ramaswamy, H.S., and Ditommaso, A. (2000) Application of artificial neural networks in image recognition and classification of crop and weeds. *Canadian Agricultural Engineering* 42(3): 147-152.

Yang, C-C., Prasher, S.O., Landry, J-A., and Ramaswamy, H.S. (2003) Development of a herbicide application map using artificial neural networks and fuzzy logic. *Agricultural Systems*, 76: 561-574.

Zwiggelaar, R. (1998) A review of spectral properties of plants and their potential use for crop/weed discrimination in row crops. *Crop Protection*, 13(3): 189-206.

APPENDIX A

8° Hemispherical spectral reflectance coefficients for 12” x 12” Spectralon panel (SRT-99-120).

Wavelength (nm)	Reflectance Coefficient
400	.987
450	.987
500	.988
550	.988
600	.988
650	.987
700	.987
750	.987
800	.990
850	.989
900	.991
950	.989
1000	.988

APPENDIX B

Single date MLC crop (CAN=yellow, PEA=green, WHT=cyan) and weed (RRP=red, WO=orange) classification output of July 19 and July 26 image data.

July 19

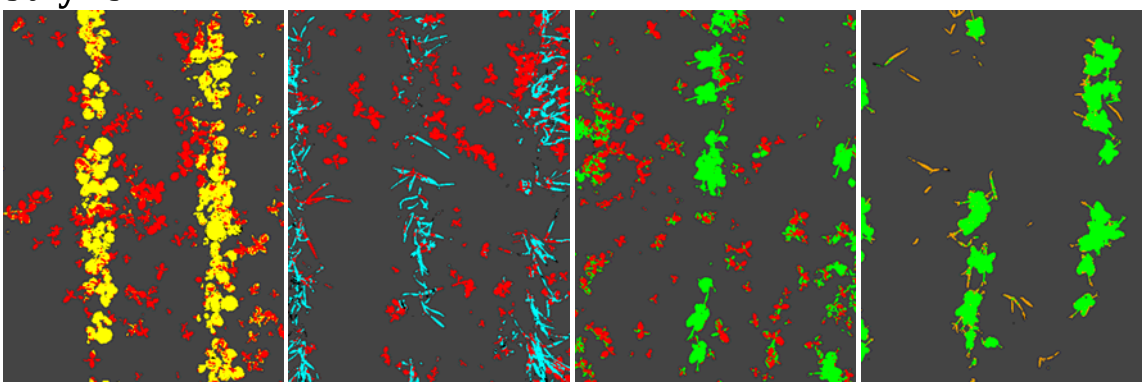

July 26

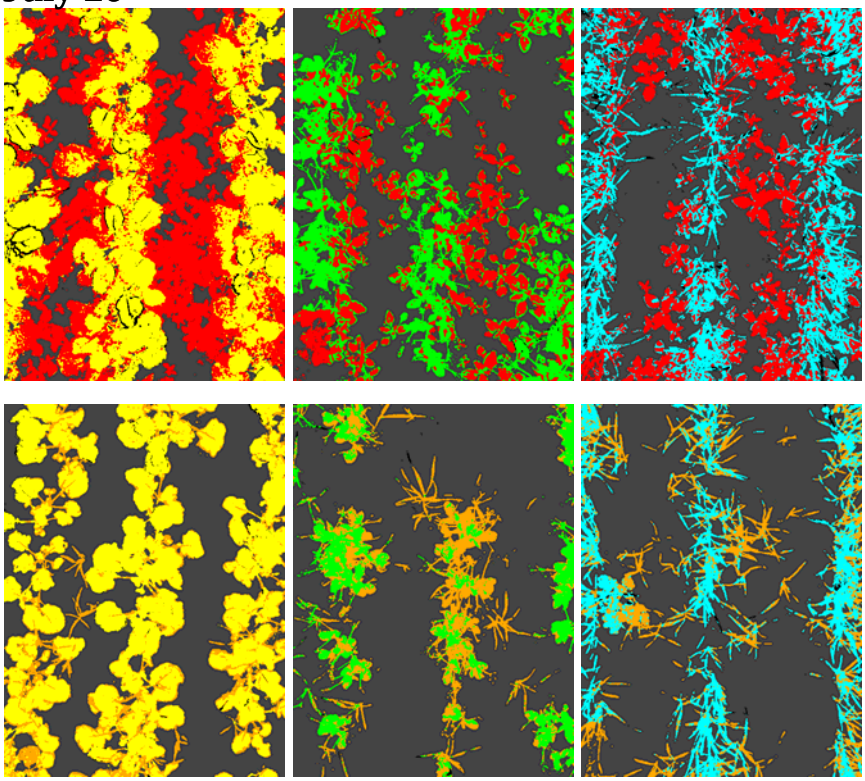

APPENDIX C

Single date ANN crop (CAN=yellow, PEA=green, WHT=cyan) and weed (RRP=red, WO=orange) classification output of July 19 and July 26 image data.

July 19

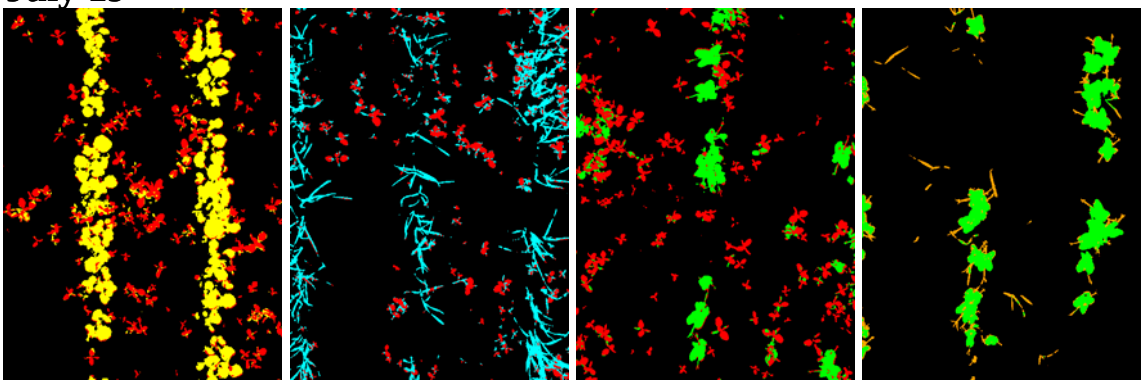

July 26

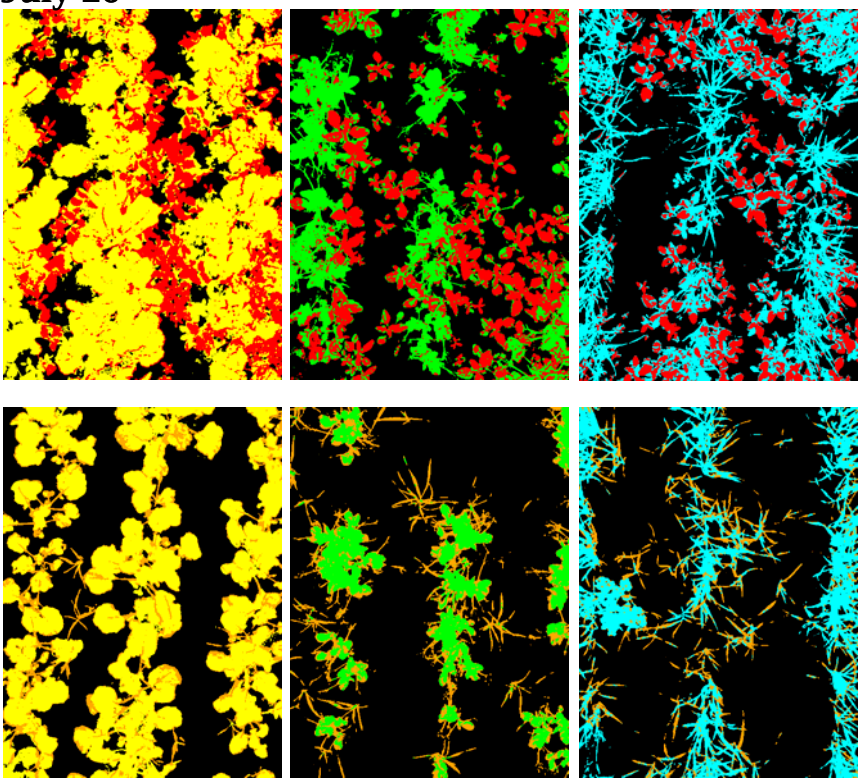

APPENDIX D

Multitemporal MLC crop (CAN=yellow, PEA=green, WHT=cyan) and weed (RRP=red, WO=orange) classification output of July 19 and July 26 image data.

July 19

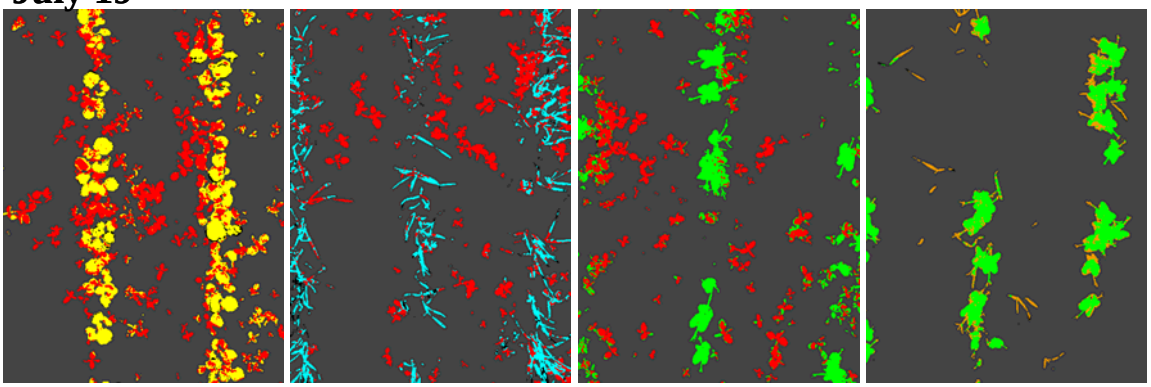

July 26

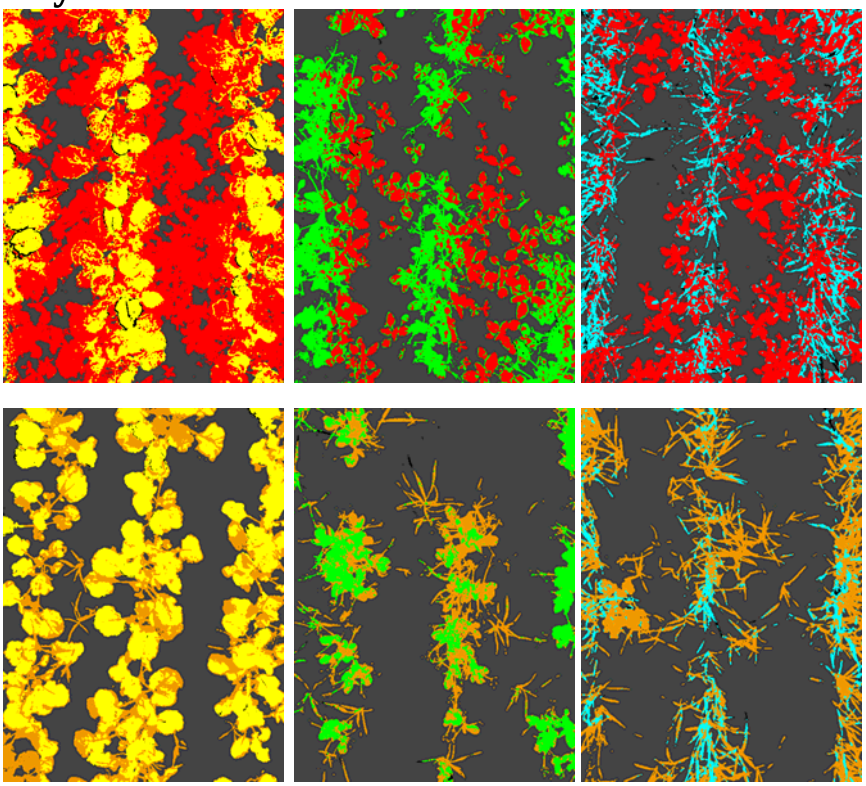

APPENDIX E

Multitemporal ANN crop (CAN=yellow, PEA=green, WHT=cyan) and weed (RRP=red, WO=orange) classification output of July 19 and 26 image data.

July 19

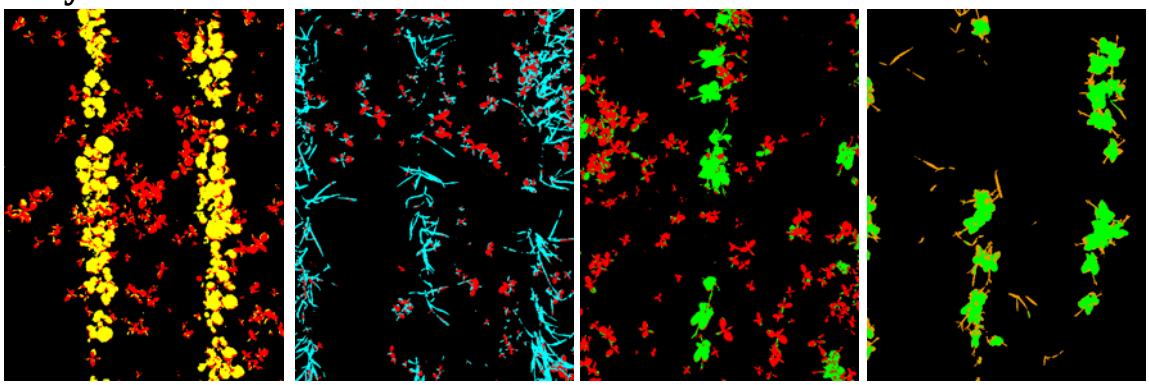

July 26